GCA-TR-67-7-N

UPPER ATMOSPHERE TEMPERATURE DETERMINATION USING AlO BANDS EXCITED BY THE SUN AT TWILIGHT

Gordon Best

Contract No. NASW-1083

May 1967

Prepared for

NATIONAL AERONAUTICS AND SPACE ADMINISTRATION
Headquarters
Washington, D. C.

TABLE OF CONTENTS

UPPER ATMOSPHERE TEMPERATURE DETERMINATION USING AlO BANDS EXCITED BY THE SUN AT TWILIGHT

By Gordon Best

INTRODUCTION

Following the failure to obtain reliable upper atmosphere temperature measurements from observations of the first resonance lines of alkali metal trails laid at twilight, several groups have examined the spectra obtained when aluminum monoxide is generated in the upper atmosphere at twilight and illuminated by the sun. In this study the details of the AlO spectrum and the methods used to interpret the band intensities in terms of temperature are reviewed, and the validity of the methods are examined.

As is well known, the electronic, vibrational, and rotational energy levels of an undisturbed molecular gas are populated according to the Boltzmann distribution:

$$N_u = N_1 \frac{g_u}{g_1} \exp\left(\frac{-E_{ul}}{kT}\right)$$

where

N_u is the number of molecules in the upper excited level,
N_1 is the number of molecules in the lower excited level,
g_u and g_1 are the statistical weights of the upper and lower levels,
E_{ul} is their energy difference,
k is Boltzmann's constant,
T is the absolute temperature.

When E is expressed in cm^{-1}, the exponent becomes

$$-E/0.6952\ T$$

Since the upper atmosphere temperatures expected are 2000°K or less, and since the energy involved in an electronic transition is much larger than the corresponding energy kT, we are chiefly concerned with the population distribution of the vibrational and rotational levels of the ground electronic state. If we assume a certain temperature we can calculate the population distribution of the vibrational and rotational levels. If now radiation of known spectral energy distribution illuminates the molecules, some will be raised temporarily to higher, excited levels. Infrared radiation will affect the population distribution of the vibrational levels of the ground electronic state. Visible radiation will excite electronic transitions. The population distribution of each vibrational and rotational level in the upper state will be determined by

the population distribution of the ground state, the radiation intensity of the wavelength corresponding to the energy difference between two particular levels, and the transition probability for transitions between these two levels. Now the lifetime of the excited state is of the order 10^{-8} sec, so the molecules will radiate almost immediately. The intensities of the lines and bands emitted will depend on the populations of the rotational vibrational levels of the upper state, and the downward transition probabilities from each level of the upper electronic state to each level of the ground electronic state. Thus, the observable spectrum corresponding to a particular gas temperature may be calculated. Comparison of the observed spectrum with the results of several such calculations will lead to an estimate of the upper atmosphere temperature.

It is obvious that as a result of excitation and emission only, the populations in the ground state will not necessarily be the same as we assumed at the beginning. Also, if the AℓO vapor cloud is optically thick, the observed spectrum may not correspond to that produced by the above process. These facts are dealt with in more detail in the discussion of synthetic spectra.

It is obvious that in order to synthesise spectra corresponding to a range of ground state temperatures, we require detailed knowledge of the AℓO spectrum, of the transition probabilities between the various pairs of energy levels, and of the intensity of solar radiation at wavelengths corresponding to these transitions.

THE SPECTRUM OF ALUMINUM MONOXIDE

Definitions

We will be concerned chiefly with the energy levels of the AℓO molecule and the wavelengths corresponding to transitions between them. First, the theory of molecular spectra in so far as is necessary for this study of the AℓO is reviewed. Further details are given by Herzberg [1]*, Feofilov [2], and Soshnikov [3].

The AℓO molecule consists of an aluminum atom and an oxygen atom bonded together. Obviously most of the mass is concentrated in the two nucleii of masses $m_{A\ell}$ and m_o on the atomic mass scale $O^{16}=16$. (It is convenient to use this scale since the observations of molecular constants used here were made before the introduction of the $C^{12}=12$ scale). Let us define the "reduced mass" of the molecule μ as

$$\frac{1}{\mu} = \frac{1}{m_{A\ell}} + \frac{1}{m_o} \quad \text{or} \quad \mu = \frac{m_{A\ell}\, m_o}{m_{A\ell} + m_o} = 10.0452 \qquad (1)$$

The electron cloud surrounding these nucleii will behave similarly to the cloud surrounding the nucleus of a single atom, and one electron will be considered available for transitions from one electronic energy level to another. Let the

* Numbers in [ ] denote reference.

energy difference corresponding to this transition be given by $E(e) = hcT_e$ ergs where T_e is expressed in units of cm^{-1}, and $hc = 1.9863 \times 10^{-16}$ erg cm.

The distance between the nucleii, r, may oscillate about a mean. From the classical theory, the frequency is

$$\nu \text{ osc} = \frac{1}{2\pi}\sqrt{\frac{k}{\mu}} \tag{2}$$

where k is the force constant for small changes in the inter-nuclear distance. According to quantum theory the energy of the molecular vibrations is quantized to a series of eigenvalues given by

$$E(v) = \frac{h}{2\pi}\sqrt{\frac{k}{\mu}}\left(v + \frac{1}{2}\right) = h\,\nu_{osc}\left(v + \frac{1}{2}\right) \tag{3}$$

where v is the vibrational quantum number. The term value is given by

$$G(v)\ (cm^{-1}) = \frac{E(v)}{hc} = \frac{\nu_{osc}}{c}\left(v + \frac{1}{2}\right) = \omega\left(v + \frac{1}{2}\right). \tag{4}$$

Similarly, the molecule may rotate about an axis perpendicular to the line joining the two nucleii. The moment of inertia about this axis is

$$I = \mu r^2 \tag{5}$$

where r is the internuclear distance. If the rotational frequency is ν_{rot}, $E(r) = 1/2\ I\ (2\pi\nu_{rot})^2$. According to quantum mechanics E(r) is quantized to eigenvalues given by (6)

$$E(r) = \frac{h^2}{8\pi^2}\frac{J}{\mu}\frac{(J+1)}{r^2} = \frac{h^2}{8\pi^2}\frac{J\ (J+1)}{I} \tag{7}$$

where J is the rotational quantum number. The term value corresponding to each of these energy levels will be

$$F(J) = \frac{E(r)}{hc} = \frac{h}{8\pi^2\ c\ I}\,J(J+1) = B\ J\ (J+1). \tag{8}$$

The magnitudes of the molecular constants are such that

$$T_e \gg G(v) \gg F(J)$$

for any one molecule, and

$$\nu_{vib} \gg \nu_{rot}$$

When the force constant k is no longer constant for vibrations of larger amplitude, i.e. the potential energy curve contains a cubic term, the term values are given by

$$\frac{E(v)}{hc} = \omega_e(v + \tfrac{1}{2}) - \omega_e x_e (v + \tfrac{1}{2})^2 + \omega_e y_e (v + \tfrac{1}{2})^3 + \ldots . \qquad (9)$$

Note that according to (4) and (9) the lowest possible vibrational level lies above the minimum of the potential energy curve. The suffix e is added since the vibrational constants depend on the potential energy curve, which in turn is a function of the electronic energy level involved.

The dissociation energy is given in units of cm^{-1} by

$D_o = \dfrac{\omega_o^2}{4\,\omega_o x_o}$ referred to lowest vibrational energy level,

$D_e = \dfrac{\omega_e^2}{4\,\omega_e x_e}$ referred to the minimum of the potential energy curve.

Molecular constants with the suffix o are measured using the lowest vibrational energy level as zero reference.

If the potential energy is represented by the Morse curve

$$U(r-r_e) = D_e [1 - \exp(-\beta(r-r_e)]^2 \qquad (10)$$

where r_e is the equilibirum internuclear distance, the vibrational energy levels are given by the term values

$$G(v) = \omega_e (v + \tfrac{1}{2}) - \frac{h\beta^2}{8\pi^2 c\mu} (v + \tfrac{1}{2})^2 \qquad (11)$$

where

$$\beta = \sqrt{\frac{2\pi^2 c\mu}{D_e h}}\,\omega_e = 1.2177 \times 10^7\, \omega_e \sqrt{\frac{\mu}{D_e}} \qquad (12)$$

When energy levels are determined by the electronic, vibrational, and rotational states simultaneously, the interactions must be taken into account.

Any energy level may be given by

$$E = E_e + E_v + E_r$$

or in term values

$$T = T_e + G + F \tag{13}$$

For G and F we may use the model of the vibrating rotator.

$$G = \omega_e(v + \tfrac{1}{2}) - \omega_e x_e (v + \tfrac{1}{2})^2 + \omega_e v_e (v+1/2)^3 + \ldots \tag{14}$$

$$F = B_v J(J + 1) - D_v J^2 (J + 1)^2 + \ldots . \tag{15}$$

where the suffix to B and to D indicates that the rotational constants are now functions of the vibrational energy level involved.

In general $D_v J^2 (J + 1)^2 \ll B_v J(J + 1) \approx F \ll G$

The dependence of B_v and D_v on the electronic state involved is given by

$$B_v = B_e - \alpha_e (v + \tfrac{1}{2}) + \ldots . \tag{16}$$

Where $$B_e = \frac{h}{8\pi^2 c\mu r_e^2} = \frac{27.98_{30} \times 10^{-40}}{\mu r_e^2}$$ as in Equation (8)

and $$D_v = D_e + \beta_e (v + \tfrac{1}{2}) + \ldots . \tag{17}$$

where $$D_e = \frac{4 B_e^3}{\omega_e^2}$$ and $\beta_e \ll D_e$

The D_e occurring in Equation (17) must not be confused with the dissociation energy given earlier.

Transitions between the energy levels given by the above term values may occur, and the spectrum will consist of a great number of lines, whose frequency (cm^{-1}) is

$$\nu = T' - T'' = (T_e' - T_e'') + (G' - G'') + (F' - F'') \tag{18}$$

where the single and double primes refer to the upper and lower states respectively. For a given electronic transition $(T_e' - T_e'')$ is a constant. But G' and G'' belong to different electronic energy levels with different ω_e and $\omega_e x_e$. G' may also be smaller than G''. Similarly, F' and F'' belong to two quite different rotational term series with different B_e and α_e.

Let us ignore for the moment the effect of rotational structure by putting F' and $F'' = 0$. Thus, we consider only the band origins. Then,

$$\nu = \nu_e + \omega_e' (v' + \tfrac{1}{2}) - \omega_e' x_e' (v' + \tfrac{1}{2})^2 + \omega_e' y_e' (v' + \tfrac{1}{2})^3 + \ldots$$
$$- \left[\omega_e'' (v'' + \tfrac{1}{2}) - \omega_e'' x_e'' (v'' + \tfrac{1}{2})^2 + \omega_e'' y_e'' (v'' + \tfrac{1}{2})^3 + \ldots\right] \tag{19}$$

or
$$\nu = \nu_{oo} + \omega_o' v' - \omega_o' x_o' v'^2 + \omega_o' y_o' v'^3 + \ldots$$
$$-(\omega_o'' v'' - \omega_o'' x_o'' v''^2 + \omega_o'' y_o'' v_o''^3 + \ldots) \tag{20}$$

Here ν_{oo} is the term independent of v' and v'', i.e. the frequency of the (0-0) band origin.

$$\nu_{oo} = \nu_e + (\tfrac{1}{2}\omega_e' - \tfrac{1}{4}\omega_e' x_e' + \tfrac{1}{8}\omega_e' y_e' + \ldots)$$
$$-(\tfrac{1}{2}\omega_e'' - \tfrac{1}{4}\omega_e'' + \tfrac{1}{8}\omega_e'' y_e'' + \ldots) \tag{21}$$

and
$$\left.\begin{aligned} \omega_o &= \omega_e - \omega_e x_e + 3/4\ \omega_e y_e + \ldots \\ \omega_o x_o &= \omega_e x_e - 3/2\ \omega_e y_e + \ldots \\ \omega_o y_o &= \omega_e y_e + \ldots \end{aligned}\right\} \tag{22}$$

The above formulae for ν [Equations (19) and (20)] refer to the band origins (zero lines) for which $J'=0$ and $J''=0$. (This transition is forbidden so the band origin may be displayed as a missing line.)

The inversion of Equation (22) gives:

$$\left.\begin{aligned}
\nu_e &= \nu_{oo} - \frac{1}{2}(\omega_o'-\omega_o'') - \frac{1}{4}(\omega_o'x_o'-\omega_o''x_o'') \\
&\quad - \frac{1}{8}(\omega_o'y_o'-\omega_o''y_o'') + \frac{1}{16}(\omega_o'z_o'-\omega_o''z_o'') \\
\omega_e &= \omega_o + \omega_o x_o + \frac{3}{4}\omega_o y_o - \frac{1}{2}\omega_o z_o \\
\omega_e x_e &= \omega_o x_o + \frac{3}{2}\omega_o y_o - \frac{3}{2}\omega_o z_o \\
\omega_e y_e &= \omega_o y_o - 2\,\omega_o z_o \\
\omega_e z_e &= \omega_o z_o
\end{aligned}\right\} \qquad (23)$$

The coefficient $\omega_o y_o \approx \omega_e y_e$ is usually very small and can be neglected. The coefficient $\omega_o z_o \approx \omega_e z_e$ is even smaller.

The isotope effect will not be considered at the moment since the abundance ratio of $O^{16}:O^{18}:O^{17}$ is 506:1:0.204, and aluminum consists of a single species $A\ell^{27}$. The term values of isotopic molecules are related by simple equations.

Multiplet Structure of Rotational Lines

So far we have seen that each electronic state consists of many energy levels, each corresponding to a different energy of vibration of the molecule. Similarly, each vibrational level is further subdivided into several energy levels each corresponding to a different energy of rotation of the molecule. In general, these will be sufficient to discuss the $A\ell O$ spectrum as observed at twilight. However, in order to discuss other aspects of the flourescence process we must consider the molecule in more detail.

The electronic oribital momentum vector $\underline{L}$ may precess about the internuclear axis. The component of this precession along the internuclear axis is a constant

of magnitude M_L $(h/2\pi)$ where M_L can have the values

$$M_L = L, L-1, L-2, \ldots\ldots, -L.$$

The angular momentum vector $\underline{\Lambda}$ represents the component of the electronic oribital angular momentum along the internuclear axis. States with the same $|M_L|$ have the same energy. We put $|M_L| = \Lambda$. The upper and lower electronic states of the AℓO molecule are both Σ states for which $\Lambda=0$. Thus, they are non-degenerate.

As for atoms, the spins of the individual electrons form a resultant $\underline{S}$, the corresponding quantum number being integral or half-integral depending on whether the total number of electrons in the molecule is even or odd. As $\underline{S}$ may precess about the internuclear axis, with a component along the axis denoted by Σ (analogous to the symbol S in atomic spectra, and not to be confused with the Σ denoting terms with $\Lambda=0$), the quantum number of the resultant electronic angular momentum about the internuclear axis is given by $\Omega = |\Lambda + \Sigma|$.

If $\Lambda \neq 0$ there are $2S + 1$ different values of $|\Lambda + \Sigma|$ for a given value of Λ, since Σ can have integral values given by $S \leq \Sigma \leq -S$. When $\Lambda = 0$ no splitting occurs, but $2S + 1$ is still referred to as the multiplicity of the state, as long as the molecule does not rotate.

When we consider the influence of rotational and electronic motions on each other, the splitting of the energy levels, if any, will depend on the degree of coupling between these two motions.

$^2\Sigma$ states belong to Hund's case (b), which is characterized by weak (or zero) coupling of $\underline{S}$ to the internuclear axis. We now introduce the vector $\underline{N}$, corresponding to the nuclear rotation. In this case $\underline{\Lambda}$ (when it is different from zero) and $\underline{N}$ form a resultant which is designated $\underline{K}$, the "total angular momentum apart from spin". The arrangement of these momentum vectors is shown in Figure 1.

K can only have values $|K| = \sqrt{K(K + 1)}$ $(h/2\pi)$ where K is integral. Since Λ is also integral it is obvious that N does not have integral values (except by accident).

When $\Lambda = 0$, the angular momentum $\underline{K}$ is identical with $\underline{N}$ and is therefore perpendicular to the internuclear axis. The quantum number K can then have all values from 0 up. The angular momenta $\underline{K}$ and $\underline{S}$ form a resultant $\underline{J}$, the "total angular momentum including spin". The possible values for J, for a given K, are

$$J = (K + S), (K + S-1), (K + S -2) \ldots\ldots (K-S)$$

Thus, each level (except when $K < S$) with a given K consists of $2S + 1$ components. Again J is half integral for an odd number of electrons (e.g. AℓO).

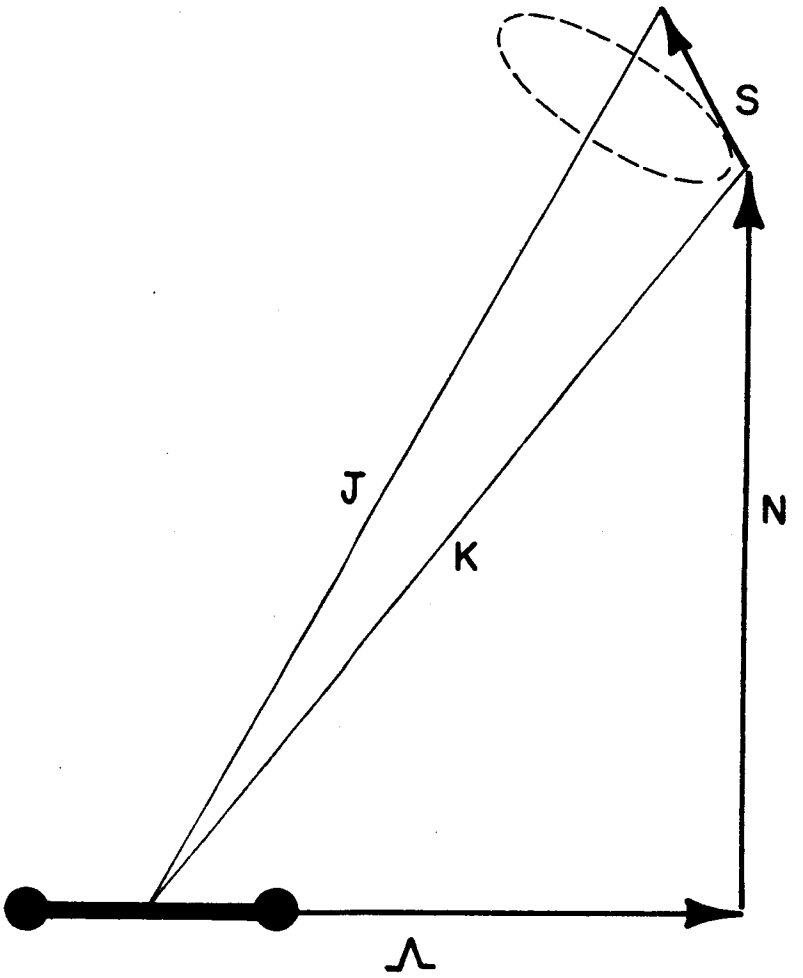

Figure 1. Molecular angular momentum vectors.

Magnetic coupling between $\underline{S}$ and $\underline{K}$ produces a slight splitting of levels with different J and equal K. When K = 0 (i.e. lowest rotational level) all Σ states are single since in this case $J \bar{\square} S$.

The rotational term values are

$$F_1(K) = B_v\, K(K+1) + \frac{1}{2}\gamma\, K \qquad \text{for } J = K + \frac{1}{2}$$

$$F_2(K) = B_v\, K(K+1) - \frac{1}{2}\gamma\,(K+1) \qquad \text{for } J = K - \frac{1}{2}$$

For a more accurate representation the term $-D_v\, K^2(K+1)^2$ should be added to each of the above. It is seen that splitting is given by $\gamma\,(K + 1/2)$ and is therefore more important for the higher rotational energy levels. Normally multiplet fine structure will not be resolved in observations of sunlit vapor trails. However, the K numbering system will henceforth be used to designate rotational levels and lines, and J will be retained as defined above.

Zeeman Effect and Polarization of Flourescence

The Zeeman effect for diatomic molecules is determined by the spatial quantization, in a magnetic field, of the total angular momentum $\underline{J}$ of the molecule. The rotational level J splits up into 2J + 1 separate energy levels, each of which is characterized by a magnetic quantum number M, where M takes on all values $-J \leq M \leq +J$. The energy difference between these magnetic levels is zero, except when a magnetic field is applied. Then the energy of a level with magnetic quantum number M differs from its unperturbed level by

$$H\bar{\mu}_H = [2\sqrt{S(S+1)}\ \cos\ (S, J)]\ \frac{M}{\sqrt{J(J+1)}}\ \mu_o H$$

for Σ states in Hund's case (b). In particular for Aℓ0, S = 1/2, cos (S, J) = $\pm$ 1 and

$$H\bar{\mu}_H = \pm\sqrt{3}\ \frac{M}{\sqrt{J(J+1)}}\ \mu_o H$$

Note that $\dfrac{M}{\sqrt{J\ (J+1)}} < 1$.

This difference will not be detected for Aℓ0 molecules generated in the Earth's magnetic field.

It is necessary to consider this degeneracy of the rotational levels in order to estimate the degree of polarization to be expected in the fluorescence emission. We shall return to this after having discussed the transitions permitted by the selection rules.

SELECTION RULES AND TRANSITION STRENGTHS

Absolute Intensities of Electronic Transitions

We may expect the total intensity of all bands associated with a single electronic transition to be of the same order of magnitude as that of an emission line resulting from an electronic transition in an atom.

The permitted transitions are determined by the symmetry properties of the electron cloud surrounding the nucleus, and by the quantum numbers Λ, Σ, and Ω describing the momenta of the molecule. In a diatomic molecule, any plane through the internuclear axis is a plane of symmetry. The electronic eigenfunction of a non-degenerate state (Σ state) either remains unchanged, or changes sign when reflected at any plane passing through both nuclei. This determines Σ^+ and Σ^- states, respectively. The selection rule here is that Σ^+ and Σ^- states cannot combine. For AℓO $A^2\Sigma$ and $X^2\Sigma$ are both + states.

The selection rules in terms of the momentum vectors are

$$\Delta\Lambda = 0, \pm 1$$

$$\Delta\Sigma = 0$$

$$\Delta\Omega = 0, \pm 1$$

For the $A^2\Sigma$ - $X^2\Sigma$ transition, $\Delta\Lambda = \Delta\Sigma = \Delta\Omega = 0$.

If we denote upper and lower states by suffices n and m, respectively, the intensity of an emission line, that is the energy emitted by the source per second, is:

$$I_{em}^{n,m} = N_n \, hc \, \nu_{nm} \, A_{nm} \quad \text{erg sec}^{-1}$$

where $hc\,\nu_{nm}$ is the energy of each quantum of wave number ν_{nm} emitted (ergs)
N_n is the number of atoms or molecules in the initial state, n
A_{nm} is the Einstein transition probability of spontaneous emission (sec^{-1}) and is defined as the rate of spontaneous emission of photons per excited atom or molecule.

Now

$$A_{nm} = \frac{64\pi^4 \nu_{nm}^3}{3h} \left|\underline{R}_{nm}\right|^2 \quad \text{for dipole radiation}$$

where $\underline{R}_{nm}$ is the matrix element of the dipole moment, and is given by

$$\underline{R}_x \text{ nm} = \int \psi_n^* M_x \psi_m \, d\tau$$

$$\underline{R}_y \text{ nm} = \int \psi_n^* M_y \psi_m \, d\tau$$

$$\underline{R}_z \text{ nm} = \int \psi_n^* M_z \psi_m \, d\tau$$

where M_x, M_y, and M_z are the components of the electric dipole moment. $|\underline{R} \text{ nm}|^2$ is known as the line strength S_{nm}

The order of magnitude of A_{nm} for strong dipole transitions is 10^8 sec^{-1}. We thus have

$$I_{em} \text{ nm} \propto \nu_{nm}^4 \left|\underline{R}_{nm}\right|^2$$

If we define absorption coefficient by the relation

$$I_\nu = I_\nu^o \exp(-k_\nu \Delta x) \simeq I_\nu^o (1 - k_\nu \Delta x + \ldots)$$

where I_ν and I_ν^o are the intensities after and before transmission through a column of length Δx of the gas at 0^oC and 1 atm pressure. The absorption coefficient k_ν varies across a line, or band. Then the intensity of the absorption for small Δx is given by

$$I_{abs} \text{ nm} = \int (I_\nu^o - I_\nu) \, d\nu = I_\nu^o \Delta x \int k_\nu \, d\nu = I_\nu^o N_m \Delta x B_{mn} hc \nu_{nm}$$

Hence

$$\int k_\nu \, d\nu = N_m B_{mn} hc \nu_{nm}$$

where B_{nm} is the Einstein transition probability of absorption, defined for energy intensity per unit frequency interval, and N_m is the number of atoms or molecules per cm^3. It is known from quantum mechanics that

$$B_{mn} = \frac{1}{8\pi\, hc\, \nu_{nm}^3} \qquad A_{nm} = \frac{8\pi^3}{3h^2 c} \left|\underline{R}_{nm}\right|^2$$

Hence, measurements of absolute transition probabilities may be based on absorption measurements. The rate of photon absorption per cm^3 is $I_{abs}/c\, h\nu_{nm} = N_m\, B_{nm}\, I_{nm}$.

The oscillator strength f_{nm} is given by

$$f_{nm} = \frac{8\pi^2\, \mu\, c\, \nu_{nm}}{3\, he^2} \left|\underline{R}_{nm}\right|^2 = \frac{\mu\, c}{8\pi^2\, e^2\, \nu_{nm}^2} A_{nm} = \frac{\mu\, hc^2\, \nu_{nm}}{\pi e^2} B_{mn}$$

$= 1.5 \times 10^{-8}\, \lambda_{nm}^2\, A_{nm}$ where λ is in microns, A is in sec^{-1}, and μ and e are the mass and charge of the electron. For a single emission electron the sum rule

$$\sum_n f_{nm} = 1$$

implies that for strong electronic transitions f may be of the order of unity.

The mean life of the excited state is given by

$$\tau = \frac{1}{A} \text{ or } \frac{1}{\sum_m A_{nm}}$$

where the level n may be depopulated by transitions to more than one lower level m.

Much confusion arises from the fact that the Einstein B coefficients may be defined in terms of energy intensity [B(I)] or terms of energy density [B(ρ)]. If ρ is the energy density per cm^3 and N_m is the number of atoms or molecules in the lower state m, the rate of excitation of atoms or molecules to the state is

$$\frac{dN_n}{dt} = N_m\, B(\rho)\, \rho$$

$$= N_m\, B(I)\, I$$

Since $I = c\rho$, it may be seen that $B(\rho) = cB(I)$. In addition the frequency of the radiation concerned may be written as $\nu(f)$ or as wavenumber $\nu(n)$, where $\nu(f) = c\nu(n)$.

$B(I)$ and $\nu(n)$ have been used throughout the preceeding discussion.

Vibrational Structure of Electronic Transitions

If the vibrating molecule behaved exactly as a perfect harmonic oscillator, only those transitions for which $\Delta v = \pm 1$ are permitted, provided the molecule has a permanent dipole moment. Once we take account of the anharmonicity of the oscillating molecule, transitions with $\Delta v = \pm 2, \pm 3$, etc become permissible. When the oscillating molecules actually correspond to two different electronic states of the same molecule, then the selection rule is no longer simple, and in fact depends on the overlap integral of the vibrational wave functions of upper and lower states.

When the electronic states are degenerate, in particular when we are concerned with the vibrational and rotational levels of each electronic state, we can write for a given rotational and vibrational transition.

$$\underline{R}_{nm} = \underline{R}_{e\ nm}\ \underline{R}_{vib\ v'v''}\ \underline{R}_{rot\ J'J''}$$

if the eigen-function can be resolved into the product of electronic, vibrational, and rotational functions, - $\psi = \psi_e\ \psi_{vib}\ \psi_{rot}$. This is known as the Born - Oppenheimer approximation.

The transition probability for absorption is then given by

$$B_{nm.,\ v''v',\ J''J'} = \frac{8\pi^3}{3h^2c} \left|\underline{R}_{e\ nm}\right|^2 \left|\underline{R}_{vib\ v'v''}\right|^2 \frac{\sum_{M'M''} \left|\underline{R}_{rot\ J'J''}\right|^2}{2\ J'' + 1}$$

where the summation is over all values of the magnetic quantum numbers M' and M''. This summation takes account of the degeneracy of J levels. If we sum the transition probability over all transitions that can occur from a given level v'', J'' we obtain the simple result

$$B_{mn} = \sum_{v'} \sum_{J'} B_{mn,\ v''v',\ J''J'} = \frac{8\pi^3}{3h^2c} \left|\underline{R}_{e\ nm}\right|^2$$

since, due to the rotational and vibrational sum rules;

$$\sum_{J'} \sum_{M'M''} \left| \underline{R}_{rot}\ J'J'' \right|^2 = 2J''+1, \quad \sum_{v'} \left| \underline{R}_{vib}\ v'\ v'' \right|^2 = 1$$

Since this result is independent of the values of v'' and J'' it follows that if the molecules are distributed over a number of lower states, the total intensity of absorption, summed over all transitions of the band system that occur, is still proportional to B_{mn}, that is, to the electronic transition probability.

In performing temperature analysis, we examine the intensity distribution of vibrational bands and rotational lines occurring in transitions between the ground and first excited electronic states. Thus, absolute values of the electronic dependence of this transition probability need not be known accurately, and the assumption that the oscillator strength associated with these transitions is less than or equal to unity is sufficient for other considerations, which need only be within an order of magnitude.

Hence, denoting $8\pi^3/3\pi^2 c \left| \underline{R}_e\ mn \right|^2$ by K and making use of the rotational sum rule, we find

$$B_{v''\,v'} = K \left| \underline{R}_{vib}\ v'\ v'' \right|^2$$

If the variation of $\underline{R}_e$ with r is slow we may write

$$\underline{R}_{vib}\ v'v'' = \int \psi_{v'}\ R_e(r)\ \psi_{v''}\ dr = R_e(\bar{r}) \int \psi_{v'}\ \psi_{v''}\ dr$$

where

$$\underline{R}_e(r) = \int \psi_e'^*\ \underline{M}_e\ \psi_e''\ d\tau_e \quad \text{(electronic transition moment)}$$

and

$$\bar{r}_{v'v''} = \frac{\int \psi_{v'}\ \psi_{v''}\ r\ dr}{\int \psi_{v'}\ \psi_{v''}\ dr} \quad \text{(r-centroid)}$$

Some authors use $\bar{R}_e$ for $R_e(\bar{r})$. More specifically, we have in emission where there are $N_{v'}$ molecules in the upper excited level v'

$$I_{em}\ v'v'' = \frac{64\pi^4 c}{3} N_{v'} \nu^4 R_e^2(\bar{r}) \left[\int \psi_{v'} \psi_{v''}\ dr\right]^2$$

and in absorption, where there are $N_{v''}$ molecules/cc in the absorbing path of length Δx

$$I_{abs}\ v'v'' = \frac{8\pi^3}{3hc} I_o \Delta x N_{v''} \nu R_e^2(\bar{r}) \left[\int \psi_{v'} \psi_{v''}\ dr\right]^2$$

Note that $I_{em}\ v'v''$ is obtained by multiplying the rate of photon emission

$$A_{v'v''} N_{v'} = \frac{64\pi^4 \nu_{v'v''}^3}{3h} N_{v'} \left|R_{v'v''}\right|^2$$

by the energy per photon, $hc\ \nu_{v'v''}$, so that I_{em} is given in erg sec^{-1}. On the other hand, for absorption, if I_o is specified in ergs cm^{-2} sec^{-1} then, I_{abs} will also be in ergs cm^{-2} sec^{-1}.

$$\begin{aligned} I_{abs}\ v'v'' &= hc\ \nu\ B\ N_{v''}\ \Delta x\ I_o/c \\ &= hc\ \nu \frac{8\pi^3}{3h^2c} N_{v''}\ \Delta x\ I_o/c \left|R_{v'v''}\right|^2 \\ &= \frac{8\pi^3}{3hc}\ I_o \Delta x N_{v''}\ \nu \left|R_{v'v''}\right|^2 \end{aligned}$$

The vibrational overlap integral square $\left[\int \psi_{v'} \psi_{v''}\ dr\right]^2$ has been called the Franck-Condon factor and is denoted by $q_{v'v''}$.

The vibrational sum rule also gives

$$\sum_{v'} \left[\int \psi_{v'} \psi_{v''}\ dr\right]^2 = \sum_{v''} \left[\int \psi_{v'} \psi_{v''}\ dr\right]^2 = 1 = \sum_{v'} q_{v'v''} = \sum_{v''} q_{v'v''}$$

that is, if the Franck-Condon factors are grouped in a Deslandres table, the sum of each vertical column or the sum of each horizontal row should equal 1. The calculation of Franck-Condon factors has been the subject of much attention by theoretical physicists. An accurate knowledge of these is required to determine the relative transition probabilities within a band system.

The Franck-Condon factors for AℓO are discussed, below in conjunction with the analysis of the vibrational transition probabilities of AℓO.

Rotational Structure of Electronic-Vibration Bands

We have seen that due to rotation each vibrational level of an electronic state is further subdivided into rotational energy levels.

The selection rule for the rotator is $\Delta J = \pm 1$, regardless of whether it is rigid or vibrating. When an electronic transition occurs, $\Delta J = 0$ is also permitted, except when $\Lambda = 0$ in both states. Then it is forbidden, or - more accurately - it is so weak as to be of little consequence except for low K values.

The selection rules for K are similar to those for J. Transitions with $\Delta K = \pm 1$ are permitted. Those with $\Delta K = 0$ are forbidden for $\Sigma - \Sigma$ electronic transitions. If we define ΔK as $\Delta K = K' - K''$, those lines with $\Delta K = +1$ are grouped so as to form what is known as the R branch, those with $\Delta K = -1$ form the P branch, of a vibrational band.

Figure 2 shows the first few rotational energy levels of any pair of vibrational energy levels in the $A^2\Sigma$ and $X^2\Sigma$ states of AℓO. Note that the splitting of the energy levels due to electronic spin is shown, levels with a common value of K being split depending on whether $J = K + 1/2$, or $J = K - 1/2$, giving the F_1 and F_2 terms of each rotational level. Also drawn are the lines permitted according to the selection rules already discussed. The dotted lines correspond to transitions for which $\Delta J = 0$, and these are very weak.

The relative line strengths of these transitions has been given by Mulliken [4], and his values are given in Figure 2. These show that in both P and R branches, components with $J = K + 1/2$ are larger in intensity than those with $J = K - 1/2$. The difference is slight for large K values, but is appreciable for low K values. The contribution from the Q branch is also appreciable at low K values.

We designate the R branch with $J = K + 1/2$ as R_1
the R branch with $J = K - 1/2$ as R_2
the P branch with $J = K + 1/2$ as P_1
the P branch with $J = K - 1/2$ as P_2
the Q branch with $J = K - 1/2 \rightarrow J = K + 1/2$ as ${}^{R}Q_{21}$
and the Q branch with $J = K + 1/2 \rightarrow J = K - 1/2$ as ${}^{P}Q_{12}$

(the latter two expressed in terms of downward transitions).

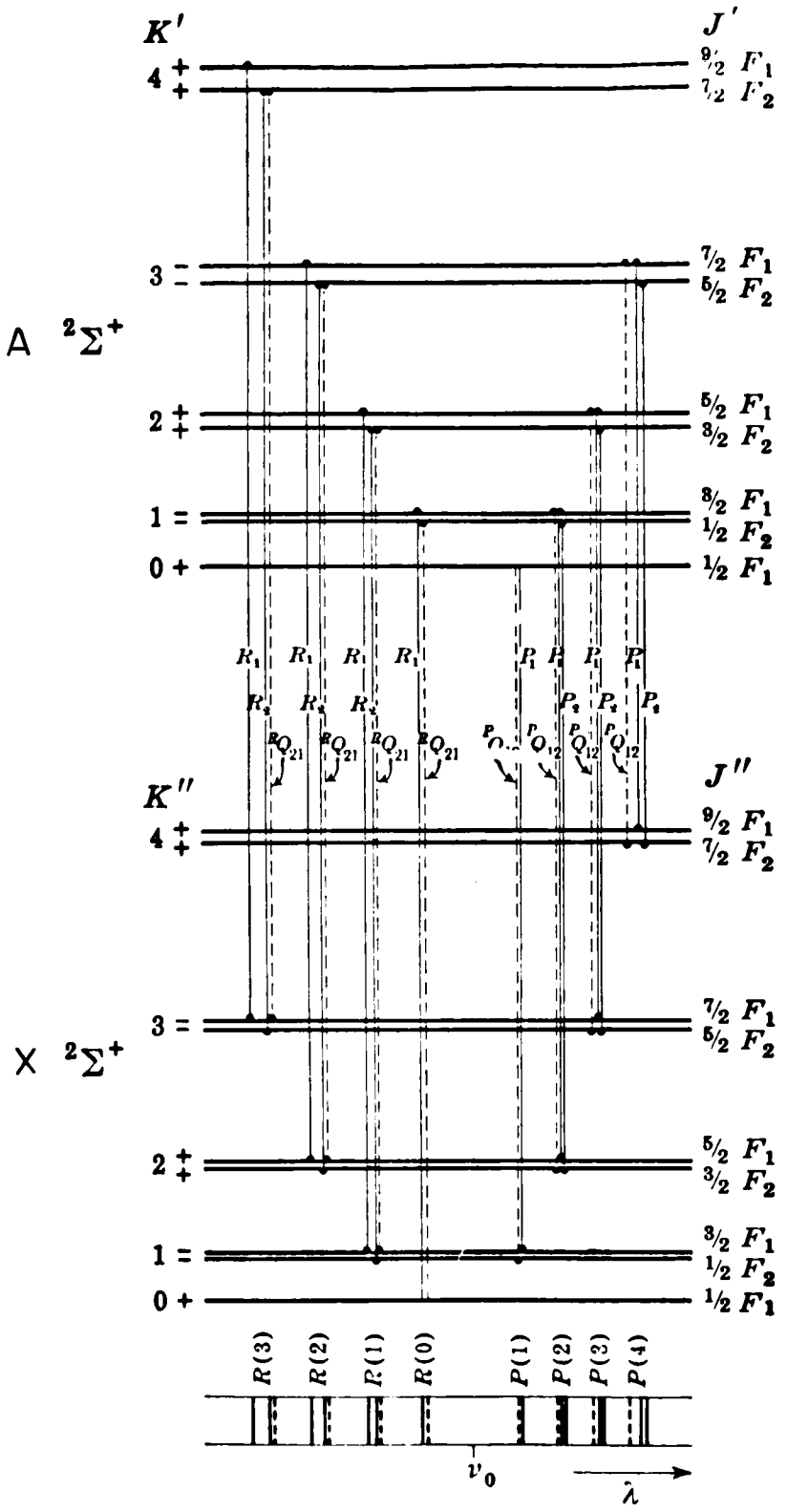

Figure 2. Some rotational levels of $A^2\Sigma$ and $X^2\Sigma$ states, and permitted transition strengths.

Selection Rules

$\Delta J = 0, \pm 1; \quad J = 0 \not\rightarrow J = 0$

$\Delta K = \pm 1$

When $\Delta J = 0$, $\Delta J \neq \Delta K$ and the intensity falls off rapidly, giving the dotted transitions.

Line Strengths (Mulliken[4])

$$S_J R = \frac{(J'' + 1)^2 - \frac{1}{4}}{J'' + 1}$$

$$S_J Q = \frac{(2J'' + 1)}{4J''(J'' + 1)}$$

$$S_J P = \frac{J''^2 - \frac{1}{4}}{J''}$$

$$S_J R + S_J Q + S_J P = 2J'' + 1$$

To obtain line strengths in terms of J', write J' for J'' in the above, and interchange $S_J R$ and $S_J P$. Hence:

$$S_J R + S_J Q + S_J P = 2J' + 1$$

If the splitting of the lines forming the P and R branches is unresolved, we may obtain their relative strengths by adding the contributions from each component, expressing them in terms of K values.

Upward transitions ($K = K''$)

$$S_K R = S\,R_1 + S\,R_2 + S^R Q_{21}$$

$$= S_J R(J = K + 1/2) + S_J R(J = K - 1/2) + S_J Q(J = K + 1/2)$$

$$= \frac{(K + 3/2)^2 - 1/4}{(K + 3/2)} + \frac{(K + 1/2)^2 - 1/4}{(K + 1/2)} + \frac{2K + 2}{4(K + 1/2)(K + 3/2)}$$

$$= 2K + 2$$

$$S_K P = S\,P_1 + S\,P_2 + S^P Q_{12}$$

$$= S_J P(J = K + 1/2) + S_J P(J = K - 1/2) + S_J Q(J = K - 1/2)$$

$$= \frac{(K + 1/2)^2 - 1/4}{(K + 1/2)} + \frac{(K - 1/2)^2 - 1/4}{(K - 1/2)} + \frac{2K}{4(K - 1/2)(K + 1/2)}$$

$$= 2K$$

Downward transitions ($K = K'$)

$$S_K R = S\,R_1 + S\,R_2 + S^R Q_{21}$$

$$= S_J R(J = K + 1/2) + S_J R(J = K - 1/2) + S_J Q(J = K - 1/2)$$

$$= \frac{(K + 1/2)^2 - 1/4}{(K + 1/2)} + \frac{(K - 1/2)^2 - 1/4}{(K - 1/2)} + \frac{2K}{4(K - 1/2)(K + 1/2)}$$

$$= 2K$$

$$S_K P = S\,P_1 + S\,P_2 + S^P Q_{12}$$

$$= S_J P(J = K + 1/2) + S_J P(J = K - 1/2) + S_J Q(J = K + 1/2)$$

$$= \frac{(K + 3/2)^2 - 1/4}{(K + 3/2)} + \frac{(K + 1/2)^2 - 1/4}{(K + 1/2)} + \frac{2K + 2}{4(K + 1/2)(K + 3/2)}$$

$$= 2K + 2$$

We may summarise these results by stating

Upward transitions

$$\text{R branch } (K' = K'' + 1),\ S_R = \frac{K'' + 1}{2K'' + 1} = \frac{K'}{2K' - 1}$$

$$\text{P branch } (K' = K'' - 1),\ S_P = \frac{K''}{2K'' + 1} = \frac{K' + 1}{2K' + 3}$$

Downward transitions

$$\text{R branch } (K' = K'' + 1)\ S_R = \frac{K'}{2K' + 1} = \frac{K'' + 1}{2K'' + 3}$$

$$\text{P branch } (K' = K'' - 1)\ S_P = \frac{K' + 1}{2K' + 1} = \frac{K''}{2K'' - 1}$$

We may estimate the relative intensities of each of the three components in the P and R branches by means of the Table 1, K being the upper value for downward transitions.

It may be seen that in both P and R branches, the component with $J = K + 1/2$, which has slightly higher energy and shorter wavelength, is also slightly more intense than the component with $J = K - 1/2$. This difference reduces with increasing values of K. This intensity difference was detected by Lagerquist et al. [5] but although Sen [6] was aware of this intensity difference, he could not detect it for the K-values for which they were resolved.

TABLE 1

RELATIVE INTENSITIES OF LINES OF P,Q AND R LINES IN AℓO BANDS

R branch		R_1	R_2	$^RQ_{21}$
P branch		P_1	P_2	$^PQ_{12}$
K	K			
1	0	0.6666	0	0.3333
2	1	0.6000	0.3333	0.0666
3	2	0.5714	0.4000	0.0286
4	3	0.5555	0.4286	0.0159
5	4	0.5455	0.4444	0.0101
6	5	0.5385	0.4545	0.0070
7	6	0.5333	0.4615	0.0051
8	7	0.5394	0.4667	0.0039

APPEARANCE OF VIBRATION-ROTATION BANDS

The energy of the electronic transition determines the general location of the band system. For AlO, T_e = 20688.95 cm^{-1} which corresponds to 4833.5Å. Therefore the system lies in the blue-green region of the spectrum.

Each band in the emission spectrum corresponds to a transition from one vibrational level in the excited electronic state to a vibrational level in the ground electronic state. Since $|\omega_e' - \omega_e''| \ll \omega_e' \simeq \omega_e''$, it is obvious that bands with equal values of Δv will be grouped together. These groups are known as sequences. If $\omega_e' < \omega_e''$, the bands in each sequence will be arranged so that bands with lower values of v' or v'' will be at the short wavelength end of the group. This is the case with AlO. Due to the higher population of levels with lower vibrational quantum number, the bands originating in the lowest vibrational levels will also be brightest.

We now consider the fine structure (due to rotation) of each band, and let the band origin be denoted by ν_o. This corresponds to the transition from the K = 0 rotational level in one vibrational level to the K = 0 rotational level in another vibrational level, which is not permitted by the selection rules. Therefore band origins are identified by a missing line.

The wavenumber of any rotation line in a band will be given by

$$\nu = \nu_o + B_v' K' (K' + 1) - B_v'' K'' (K'' + 1)$$

When $\Delta K = +1$ we obtain the R branch of the band:

$$\nu_R = \nu_o + 2 B_v' + (3 B_v' - B_v'') K + (B_v' - B_v'') K^2; \quad K = 0,1...$$

When $\Delta K = -1$ we obtain the P branch of the band:

$$\nu_P = \nu_o - (B_v' + B_v'') K + (B_v' - B_v'') K^2; \quad K = 1,2....$$

where K″ has been replaced by K and $\Delta K = K' - K''$.

Due to the quadratic term in the above, one of the branches turns back, forming a band head. A head is formed in the R branch if $B_v' - B_v'' < 0$ and the band is degraded toward the red. Conversely when $B_v' - B_v'' > 0$, the band head is in the P branch and it is degraded toward the blue. The P and R branches may be represented by a single formula

$$\nu = \nu_o + (B_v' + B_v'') m + (B_v' - B_v'') m^2$$

where m = -K for the P branch and m = K + 1 for the R branch.

Then the m value at the band head may be found to be

$$m_{head} = - \frac{B_v' + B_v''}{2(B_v' - B_v'')}$$

and the wavenumber separation between the band origin and the head is given by

$$\nu_{head} - \nu_o = \frac{-(B_v' + B_v'')^2}{4(B_v' - B_v'')}$$

For AℓO, $B_v' - B_v'' < 0$, so the heads are formed in the R branches, and the bands are degraded toward the red. Inserting approximate values for B_v' and B_v'' we find that the turning point occurs at about K = 17, and is about 2.5Å away from the band origin. In contrast, the separation of adjacent band origins is given approximately by $(\omega_e' - \omega_e'')$ and this corresponds to about 25Å. Figure 3 shows how the wavelengths of the rotational lines in the bands of the $\Delta v = -1$ sequence vary with both the initial rotational quantum number and the initial vibrational quantum number. The wavelengths were calculated at intervals ΔK = 20 up to K′ = 140. It may be shown that the K value at which the returning R branch reaches the band origin is equal to twice the K value at the head, or for AℓO, a value of 33.

Since, for the range of temperatures to be met, the relative population of the rotational levels peaks in the region K″ = 10 to 20, the band will consist of a pair of peaks, that of the R branch being higher, because it returns at about K = 17 and overlaps itself.

It may be shown that the separation of the rotational lines is given by

$$\frac{d\lambda}{dm} \text{ (Å)} = 0.31141 - 0.01865\ m$$

Thus the separation of lines of low rotational quantum number is about 0.3Å, and at K = 15 in the P branch it is about 0.6Å.

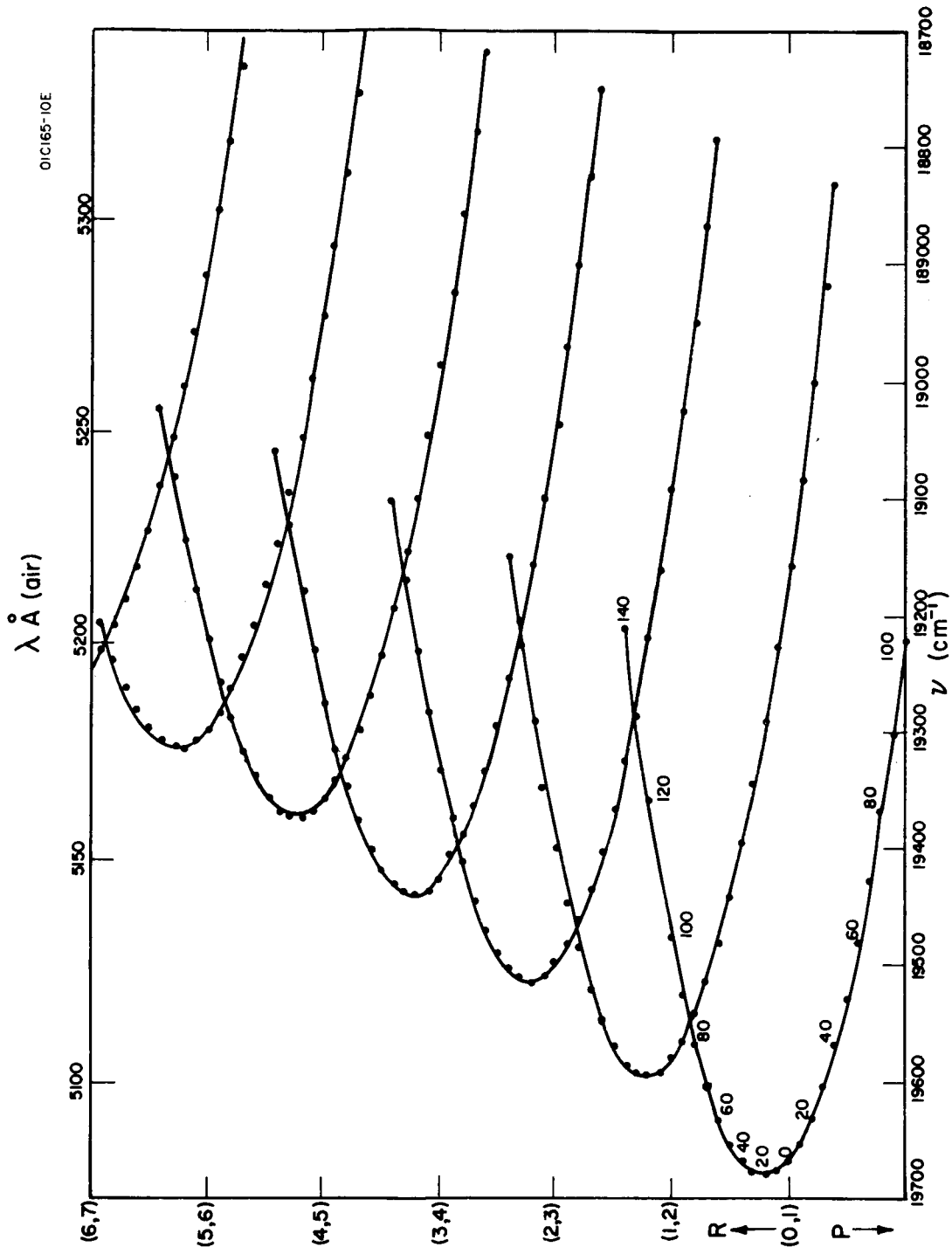

Figure 3. Wavelengths of rotational lines in $\Delta v = 1$ sequence.

OBSERVATIONS OF THE AℓO SPECTRUM

Term Values and Molecular Constants

If the wavelengths of the individual lines of each band were to be given, a table of several hundred entries would be needed. It is simpler to represent the frequencies of the lines by equations of the form discussed above, and to tabulate the necessary molecular constants. Several observations of the AℓO spectrum have been made, and the constants determined are given in Table 2. Note that some of the measurements were made without resolving the rotational structure and thus, the $\omega_e x_e$ values given refer to the band heads. The following references and comments apply to Table 2.

W.C. Pomeroy [7]

(a) ω_e was calculated using $\omega_o = \sqrt{-4 \frac{B_o^3}{D_o}}$

(b) Pomeroy used Birge's values for these

(c) He assumes that rotational energy levels are given by

$$E = B_v m^2 + D_v m^4 \ldots \text{ where m is the rotational "running number"}$$

(This is a pre-quantum mechanics treatment.) Quantum mechanics defines B_v and D_v so that $E = B_v J(J+1 + D_v J^2(J+1)^2 + \ldots$

The dependence of B and D on v is given in Pomeroy's [7] theory by

$$B_v = B_e - \alpha_e(v + 1/2) \qquad D_v = D_e + \beta_e(v + 1/2)$$

Thus, we may expect Pomeroy's determination of α and β to be correct, but not the values given for B_e and D_e.

Pomeroy lists frequencies of rotational lines in the (0,0) band ($19 \leq J \leq 142$), the (0,1) band ($6 \leq J \leq 75$) and the (1,0) band ($19 \leq J \leq 85$). Pomeroy found the spin-splitting constant γ to be 0.014 or 0.016 depending on the band involved.

W. Jevons [8] refers to:

(a) G. Ericksson and E. Hulthen [9]

(b) W.C. Pomeroy [8], above.

M.K. Sen [6]

This paper lists wave numbers of each component of the rotational lines of the (1,0), (1,1), (2,1), (0,0), (0,1) and (1,2) bands. The gives the following

TABLE 2

SPECTROSCOPIC MOLECULAR CONSTANTS FOR AlO

Author	State	T_e	ω_e	$\omega_e x_e$	B_e	α_e	D_e	β_e	r_e (Å)	ν_{oo}
Pomeroy [7]	$A^2\Sigma$		866(a)	3.75(b)	0.6019(c)	0.00453(c)	-1.1630×10^{6}	$+0.0059\times10^{-6}$	1.665	20635.27
	$X^2\Sigma$		969(a)	7.00	0.6386	0.00575	-1.1094×10^{-6}	-0.0087×10^{-6}	1.617	---
Jevons [8]	$A^2\Sigma$	20686.9	868.15	3.76	0.6019	0.00453			1.663	20635.3
	$X^2\Sigma$		977	7.00	0.6386	0.00575			1.614	
Sen[6]	$A^2\Sigma$				0.60417		-1.1660×10^{-6}		1.664	
	$X^2\Sigma$				0.64148		-1.1050×10^{-6}		1.615	
Roy[10]	$A^2\Sigma$	20699.25	870.0	3.80						
	$X^2\Sigma$		978.2	7.12						
Herzberg [1]	$A^2\Sigma$	20699.2	870.0	3.80	0.60417	0.00453			1.6667	20635.3
	$X^2\Sigma$		978.2	7.12	0.64148	0.00575	-1.114×10^{-6}	0.0087×10^{-6}	1.6176	
Lagerqvist [5]	$A^2\Sigma$	20688.95	870.05	3.52	0.60408	0.00447	-1.16×10^{-6}		1.6668	20635.18
	$X^2\Sigma$		979.23	6.97	0.64136	0.00580	-1.08×10^{-6}	-0.02×10^{-6}	1.6176	

values of the spin-coupling constant for the first three vibrational levels of the upper and lower electronic states.

v	γ'	γ''
0	0.0303	0.0211
1	0.0329	0.0197
2	0.0340	0.0162

D. Roy [10]

He lists wavelengths of band heads for v′ up to 10 and $+ 4 < \Delta v < - 3$.

G. Herzberg [1] refers to:

(a) W.C. Pomeroy above

(b) D. Roy above

(c) M.K. Sen above

A. Lagerqvist, N.E.L. Nilsson, and R.F. Barrow [5]

Lists band origins for v′ up to 3 and $2 \leq \Delta v \leq - 2$

A tabulation of band heads has been given by Shimauchi [11], who extends that given by Roy [10] to v′ = 16 and v″ = 12, but with no greater accuracy.

Vibrational Transition Probabilities

Theoretical. Calculations of vibrational transition probabilities have been made by several methods which depend mainly on the form assigned to the vibrational oscillator. This may be

(a) Simple parabolic (harmonic oscillator)

(b) Perturbed parabolic (anharmonic oscillator)

(c) Morse potential energy curve

(d) True potential energy curve based on observed molecular constants

Mannenback [12,13] has given a simple method of calculating Franck-Condon factors for a parabolic potential well model. Values of q(v′v″) obtained by this method have been used by Armstrong [14]. Bates [15] has published a set of tables allowing the evaluation of Franck-Condon factors in both the harmonic oscillator case and in the case where a non-linear term is introduced. Franck-Condon factors have also been evaluated using these, and there is fair agreement

with the results given by the Mannenback method. The most realistic analytical model of the internuclear potential is given by the Morse curve, and calculations of Franck-Condon factors for AℓO using this model have been made by Nicholls [16].

Excellent agreement with Nicholls' results was obtained by Tawde and Korwar [17], using the numerical integration method of Bates [18], also based on the Morse potential curve.

Sharma [19] has recently calculated Franck-Condon factors using potential energy curves derived from the observed vibrational energy levels. The difference between his results and those of Nicholls is small for q(0,0) but increases with v′ and v″.

Experimental. The lack of agreement among the theoretical values of q(v′v″) is greatly exceeded by the lack of agreement among the experimental observations. Quantitative measurements of band intensities have been made by Tawde and Kowar [20], and by Hébert and Tyte [21,22]. One simple test of reliability which may be applied to these is based on the following. No matter by what means the molecule is raised to the excited electronic state, the relative intensities of bands originating at a common vibrational level should be constant. The means of excitation only determines the relative populations of the vibrational levels of the excited electronic state. Expressed more briefly, the relative transition probabilities, and hence the relative intensities, in any v″ progression (horizontal row of a Deslandres table) should be independent of the means of excitation. Table 3 shows the failure of this test as applied to the observed relative intensities. The last line gives relative vales of $q(v'v'')\ \nu^4$, based on Sharma's values of q(v′v″).

TABLE 3

RELATIVE INTENSITIES OBSERVED IN v″ PROGRESSION v′ = 0 of AℓO

Experimenters	Source	Vibrational Temperature °K	0-0	0-1	0-2
Hébert and Tyte	AC arc	2900	100	9.4	0.5
Tawde and Korwar	DC arc	5000	100	13.7	---
Tyte and Hébert	Shock Tube	3600	100	23.0	1.2
Tyte and Hébert	Expl Foil	5800	100	38.0	1.1
---	$q\ \nu^4$	--	100	27.666	2.851

The lack of agreement between theoretical Franck-Condon factors and observed transition strengths may be accomodated if the electronic transition moment R_e is considered as a function of the upper and lower vibrational levels involved, - in particular as a function of the r-centroid $\bar{r}_{v'v''}$. Tawde and Korwar [23] find this variation to have the form

$$R_e = \text{const}\ (1 - 1.093)\ \bar{r})$$

using relative intensities integrated over the entire band and

$$R_e = \text{const } (1 - 0.457\ \bar{r})$$

using peak intensities. On the other hand Hebert and Tyte [21], using relative integrated band intensities find

$$R_e = \text{const } (1 - 0.46\ \bar{r})$$

Since considerable smoothing was used to obtain both the comparable results, and since the original intensities do not respond to the test for relative values in a v″ progression, the situation must be regarded as inconclusive. It is believed that self-absorption was present in some of the observations, which could account for the scatter in relative intensities [24]. A variation of band strength with current density has been observed for the nitrogen second positive system [25].

THE SOLAR SPECTRUM

In order to calculate the rates of population of the vibrational and rotational levels of the $A^2\Sigma$ state, it is necessary to know the relative intensities of the solar spectrum at wavelengths corresponding to the upward transitions. A solar spectrum with a resolution of 0.01 to 0.02Å has been given by Minnaert et al [26]. However, this gives the intensities of the absorption features (solar and terrestrial) relative to the continuum radiation. Of more importance to the current problem, this spectrum was obtained using only light from a small spot in the center of the solar disc. It may be expected that although the same features will be present in the spectrum of light from the integrated disc of the sun, the profiles will change An example of this may be found by comparing the first few Angstroms found in the main body of the Utrecht Atlas, with the last few Angstroms of the ultraviolet, found in the appendix to the Atlas. The ultraviolet was taken in integrated sunlight. However, this difference could also be due to a larger bandpass being used in the ultraviolet spectrograms. The bandpass for the ultraviolet spectrograms is not given in the Utrecht Atlas, but an investigation of the profiles of the sodium D-lines across the face of the solar disc by Priester [27] shows that absorption features do indeed become deeper and narrower as the disc is traversed from center to limb.

Many spectra in the integrated light of the solar disc have been taken at much lower resolution, the purpose being the measurement of the solar constant. Dunkelman and Scolnik [28] made measurements in 1951 with bandwidths ranging from 10Å at 3030Å to 170Å at 7000Å. The bandpass at 5000Å was probably 40-50Å. In 1955, Stair and Johnston [29] carried out a similar measurement, the intensity being measured at intervals of 30-90Å in the wavelength region 4000-6000Å.

Johnson [30] has reviewed all the data obtained by the Smithsonian Astrophysical Observatory, and incorporated with it the ultraviolet observations of Johnson and Tousey [31] and the visible observations of Dunkelman and Scolnik [28].

Spectra of the central spot of the solar disc have been evaluated on an absolute scale by Canavaggia et al. [32] and by Labs [33]. Their values refer to the radiated intensity at the solar surface, but in this report they are normalized to equal those of Johnson [30] at 5000Å.

All these results, along with the tabulation by Allen [34] have been plotted in Figure 4. It may be seen that the results of Dunkelman and Scolnik and of Johnson are in good agreement above 4500Å. Notice that the data obtained using only the central spot is relatively higher below 5000Å and relatively lower above 5000Å. Further comments on this point are included in the discussion of vibrational spectra.

Measurements of the solar spectrum were made in October 1965 from Fort Churchill at various solar zenith angles. Although the latitude, altitude, and time of year were by no means suitable for obtaining accurate, absolute solar intensities it was possible to examine the solar spectrum with a bandpass of 2.4Å, so as to seek any strong Fraunhofer lines in integrated-disc light. A few spectra were taken with the sun imaged on the entrance slit plane so that

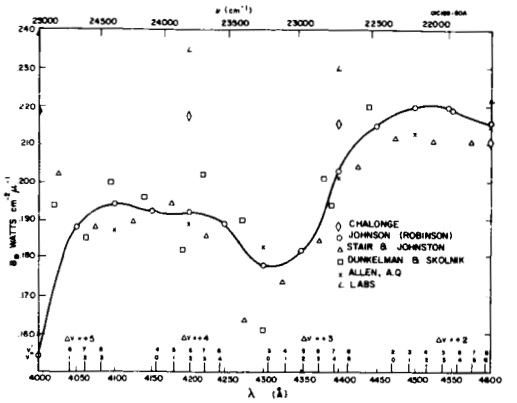

(a)

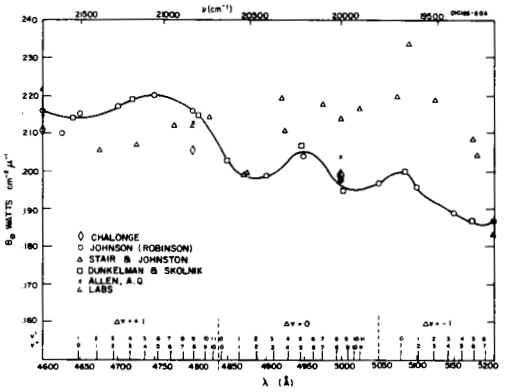

(b)

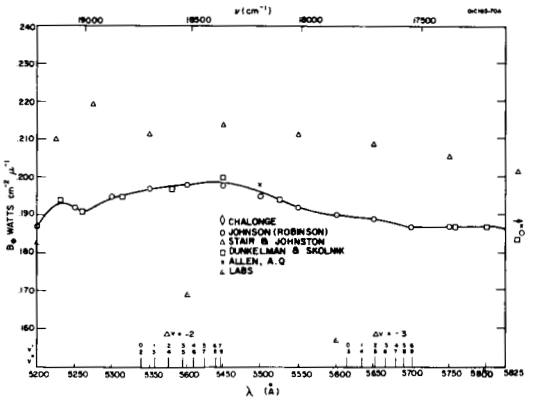

(c)

Figure 4. The solar spectrum.

TABLE 4

ABSORPTION FEATURES OF THE SOLAR SPECTRUM IN THE WAVELENGTH RANGE 4600 to 5270Å

Wavelength (Å)	Half Width (Å)	Depth (%)	Interference		Nearest Band Origin (Aℓ0)	Feature Origin
4647.4	5	5		*	(1,0)4650.25	Fe
4654.5	3	2		*	(1,0)4650.25	Fe
4667.5	6	10	*		(2,1)4674.02	Fe,Ni,Ti,Cr
4680.5	5	3		*	(2,1)4674.02	Ce,Fe,Cr,W
4703.0	7	5		*	(3,2)4696.51	Mg
4709.0	3	5			(4,3)4717.68	Ti,Fe,Cr,Mn
4715.0	3	2		*	(4,3)4717.68	Ni
4730.0	5	4			(5,4)4737.49	Fe,V,Cr
4756.0	5	3		*	(6,5)4755.91	Cr,Ni
4763.0	7	3		*	(6,5)4755.91	Mn,Zr,Ni
4786.5	10	2			(8,7) ---	Fe,Ni,V
4823.5	3	2			(10,9) ---	Mn,Cr,V
4861.4	6	20	*		(0.0)4844.74 (1.1)4868.87	H_β
4871.5	3	5		*	(1,1)4868.87	Fe
4891.5	6	8	†	*	(2,2)4891.59	Fe
4903.3	5	1			(3,3)4912.86	Fe
4910.3	4	5		*	(3.3)4912.86	Fe
4920.5	7	10	*		(3,3)4912.86	Fe
4934.0	2	4		*	(4,4)4932.64	Fe,Ba
4939.0	4	7			(5,5)4950.88	Fe,Ti
4957.5	4	10			(6,6)4967.55	Fe
4984.0	6	8	†	*	(7,7)4982.63	Fe,Ni
5007.3	2	4			(9,9) ---	Ti,Fe
5041.8	6	8			(13,13)---	Ca,Fe,Ni
5065.0	3	2			(0,1)5082.49	Ti, Fe

TABLE 4 (continued)

Wavelength (Å)	Half Width (Å)	Depth (%)	Interference		Nearest Band Origin (AℓO)	Feature Origin
5080.0	6	4		*	(0,1)5082.49	Ni,Fe
5099.0	5	6		*	(1,2)5105.42	Fe,Ni
5167.4	5	15	*	*	(4,5)5164.40	Mg,Fe
5172.7	5	16	*		(5,6)5180.65	Mg
5183.6	6	14	*	*	(5,6)5180.65	Mg
5208.5	8	4			(7,8) ---	Cr,Fe
5217.2	6	4			(8,9) ---	Fe
5227.0	4	7			(9,10) ---	Ti,Cr,Fe
5266.8	2	5			--- ---	Fe,Ti

TABLE 5

WAVELENGTH DIFFERENCE (Å) OF BAND HEAD, ORIGIN AND K′ = 15
ROTATIONAL LINES FOR THE NINE MOST INTENSE BANDS OF AℓO

Branch	⊂R ⟶		— P ⟶	
Band	Head	K′ = 15	Origin	K′ = 15
0-1	-3.2	-3.0	0	+7.1
1-2	-3.3	-3.1	0	+7.1
2-3	-3.4	-3.1	0	+7.0
0-0	-2.5	-2.4	0	+6.9
1-1	-2.5	-2.5	0	+6.9
2-2	-2.6	-2.5	0	+6.7
1-0	-2.0	-2.0	0	+6.5
2-1	-2.0	-2.0	0	+6.5
3-2	-2.1	-2.1	0	+6.5

the light investigated came from a band across the solar disc. Most spectra were obtained with a paper diffuser in front of the telescope so that light from the entire disc was examined. Tests showed that the paper was non-polarizing, achromatic, and that the contribution from skylight was negligible. Measurements were made with a polaroid both parallel to and perpendicular to the grating rulings, and without the polaroid. A bandwidth of 2.4Å corresponds to the smallest slit width that could be calibrated using the 4916Å line of mercury. Several spectra were taken with the slit much smaller and showed no significant change in solar spectrum. The 2.4Å corresponds to a slit width of less than 0.1 mm and the slit width is not calibrated below 0.1 mm.

The spectrum showed considerably less structure than the light from the central spot of the solar disc. The only significant absorption features over the wavelength range from 4600Å to 5270Å are given in the Table 4 along with estimates of half width, depth, and origin. Also tabulated are the nearest band origins of Aℓ0.

Table 5 shows the positions of the head and the rotational lines $K' = 15$ of both P and R branches relative to the origin for the first three bands of each of the $\Delta v = 0, \pm 1$ sequences. By comparing this table with the wavelength difference between the absorbing feature and the nearest Aℓ0 band origin, it was possible to select lines which, on the basis of wavelength alone, could interfere with the assumed solar spectral distribution. These are marked with asterisks in the right-hand "Interference" column. In the left-hand "Interference" column, we have marked with an asterisk those absorption features showing an equivalent width of greater than 0.5Å. Only those features marked with an asterisk in both columns may be considered serious interferences, and it is seen that this occurs only for relatively high values of v', for which the population is low for low to moderate temperatures.

The most prominent absorption feature, H_β, at 4861.3Å corresponds to the following lines

0 - 0 R branch, $K' = 63$

P branch, $K' = 29$.

Since transitions for which $\Delta K = \pm 1$ may occur, the following rotational lines will be affected in emission

R branch $K' = 63$ $K' = 29$

P branch $K' = 63$ $K' = 29$.

These are sufficiently far away from the band head for relative intensities of band heads to be unaffected. However relative integrated band intensity measurements will be affected, to a degree which depends on the temperature. In view of the many other uncertainties involved it would seem unnecessary to make any allowance for Fraunhofer absorption features at this stage.

CALCULATION OF SYNTHETIC SPECTRA

Relative Populations of Vibrational and Rotational Levels in the Ground State

According to the Maxwell-Boltzmann distribution law the population of levels with energy E is proportional to exp(-E/kT) where k is Boltzmann's constant and T is the absolute temperature. When E is expressed in cm^{-1} this becomes

$$N(E) \propto \exp\ (E/0.6952T)$$

Obviously, the proportion of AℓO molecules raised to the $A^2\Sigma$ state by thermal excitation at upper atmosphere temperatures will be negligible.

If we have a series of vibrational levels with energies G(1), G(2), G(3), etc. then the proportion of molecules in these energy levels will be

$$N(v'') = N \frac{\exp\ [-G(v'')/0.6952T]}{Q_v}$$

where

$$Q_v = \sum_{v''} \exp\ [-G(v'')/0.6952T]$$

Values of G(v'') tabulated by Tyte and Nicholls [35] have been used to determine the relative populations of the vibrational levels in the ground state of AℓO. These are shown in Figure 5 for temperatures between 200 and 5800°K.

Due to the statistical weight (2K + 1) of the rotational levels with quantum number K, the number of molecules N_K in the rotational level K is proportional to

$$(2K + 1) \exp \left[-F(K) \frac{hc}{kT}\right]$$

Expressing F(K) alternately, we may write

$$N_K \propto (2K + 1) \exp \left[-B_v\ K(K + 1) \frac{hc}{kT}\right]$$

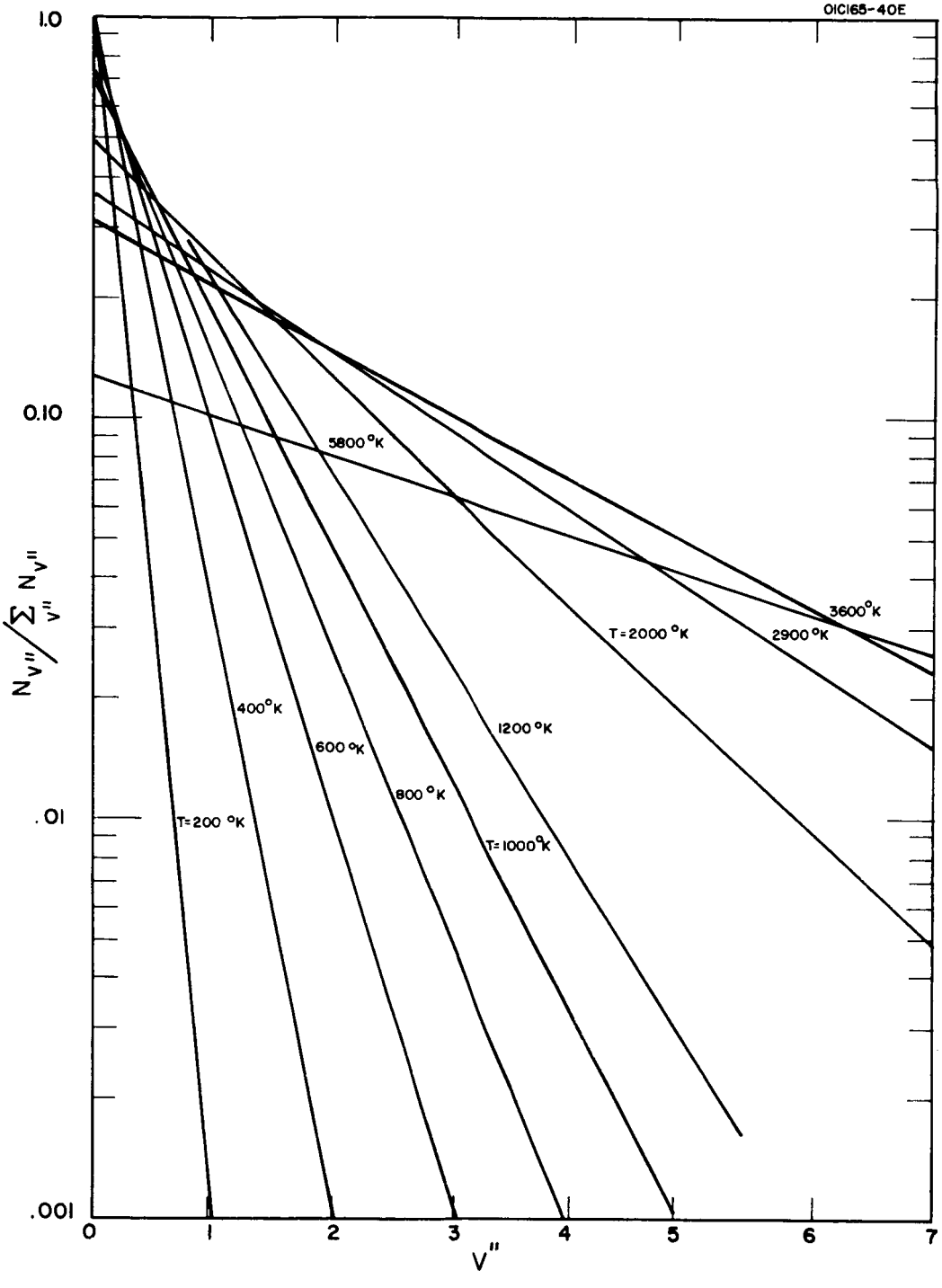

Figure 5. Relative populations of vibrational levels at various temperatures.

The actual number of molecules in rotational level K is given by

$$N_K = N \frac{2K + 1}{Q_r} \exp \left[- B_{v^-} K(K + 1) \frac{hc}{kT} \right]$$

where N is the total number of molecules (in vibrational level v') and Q_r is the rotational state sum.

$$Q_r = \sum_{K=0}^{\infty} (2K + 1) \exp \left[- B_{\nu} K(K + 1) \frac{hc}{kT} \right]$$

For sufficiently large T/B the sum may be replaced by an integral

$$Q_r \simeq \int_0^{\infty} (2K + 1) \exp \left[- B_v K(K + 1) \frac{hc}{kT} \right] dK = \frac{kT}{hcB}$$

N_K is plotted in Figure 6 for the $v'' = 0$ level of Aℓ0 at several temperatures and goes through a maximum value at K_{max}. It may be shown that

$$K_{max} = \sqrt{\frac{kT}{2\ hcB}} - 1/2 = 0.5896 \sqrt{T/B} - 1/2$$

Figure 6 also shows that if we are to consider 1 percent accuracy as desirable we must consider K values up to 35 for 200°K, 85 for 1000°K and 120 for 2000°K, so as to allow for the effects of overlap of the P branch by the R branch.

Calculation of Vibrational Spectra

The method of calculation of the synthetic spectra is quite simple. We start with a particular assumed temperature, and calculate the relative populations of the various vibrational levels of the lower state at this temperature. Here we have used the valuesof G(v″) tabulated by Tyte and Nicholls [35]. We can then determine the rate of population, by absorption of solar photons, of each of the vibrational levels of the upper state from each of the vibrational levels of the lower state. These are best arranged in a Deslandres table so that the sum of a horizontal row will yield g(v′), the rate of population [36] of vibrational level v′.

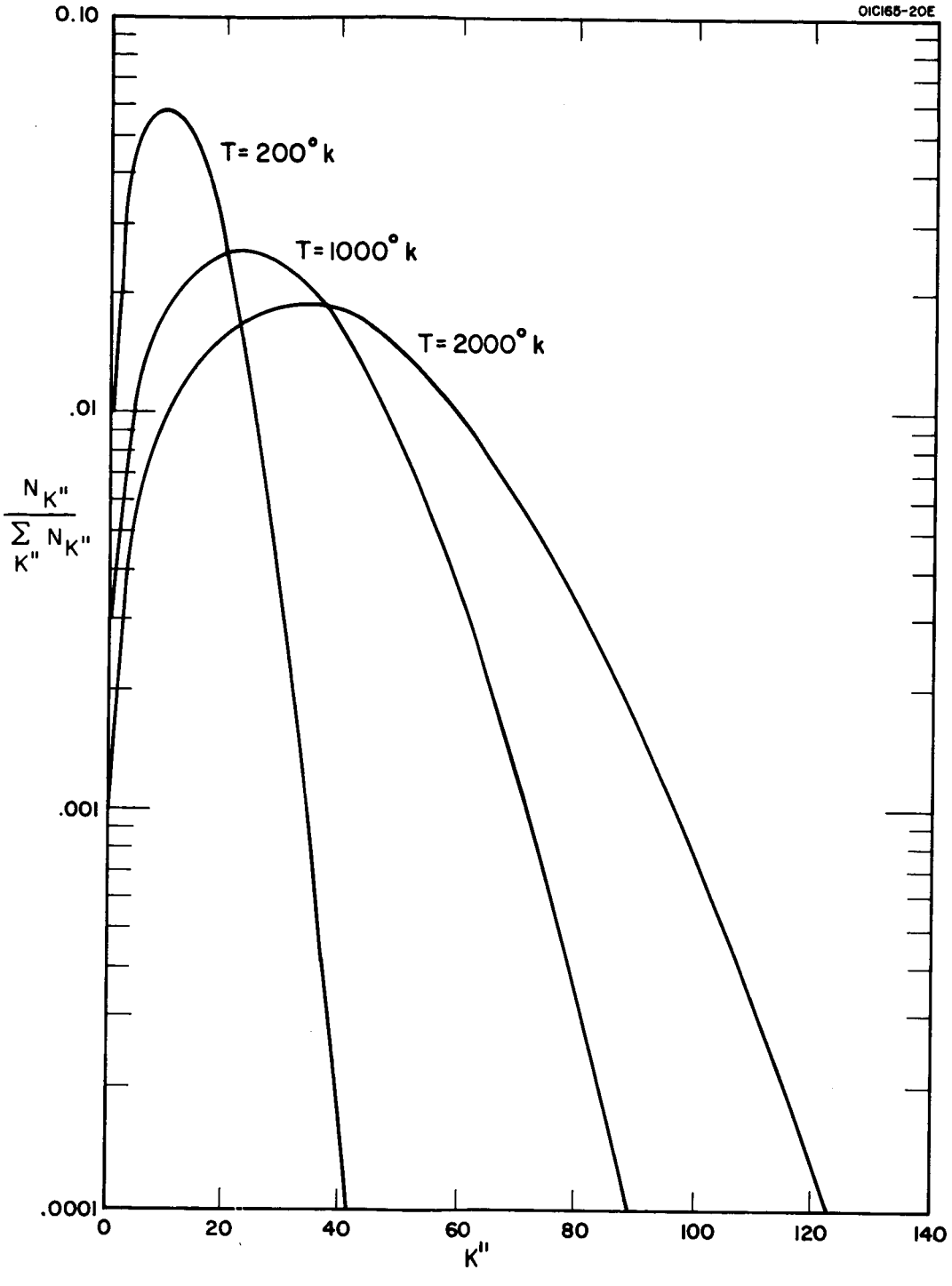

Figure 6. Relative populations of rotational levels at several temperatures (for v″ = 0).

$$g(v') = \sum_{v''} N(X,v'')\ B(A,v';\ X,v'')\ I_{\odot}(A,v';\ X,v'')$$

$$= \sum_{v''} N(X,v'')\ \frac{8\pi^3}{3h^2c}\ R_e^2(\bar{r})\ q_{v'v''}\ I_{\odot}(A,v';\ X,v'')$$

The rate of depopulation of level (A,v') is

$$a(v') = \sum_{v''} N_{v'}\ A(A,v';\ X,v'')$$

$$= N_{v'} \sum_{v''} \frac{64\pi^4}{3h}\ \nu^3\ (A,v';\ X,v'')\ R_e^2(\bar{r})\ q_{v'v''}$$

At equilibrium these rates are equal; therefore,

$$N_{v'} = \frac{g(v')}{\frac{64\pi^4}{3h} \sum_{v''} \nu^3(A,v';\ X,v'')\ R_e^2(\bar{r})\ q_{v'v''}}$$

$$= \frac{1}{8\pi hc} \frac{\sum_{v''} N(X,v'')\ R_e^2(\bar{r})\ q_{v'v''}\ I_{\odot}(A,v';\ X,v'')}{\sum_{v''} \nu^3(A,v';\ X,v'')\ R_e^2(\bar{r})\ q_{v'v''}}$$

Therefore the rate of photon emission in the transition

$$(A,v') \rightarrow (X,v'')$$

is

$$a(v'-v'') = N_{v'}\, A(A,v';\ X,v'')$$

$$= \frac{g(v')\ \nu^3(A,v';\ X,v'')\ R_e^2(\bar{r})\ q_{v'v''}}{\sum_{v''} \nu^3(A,v';\ X,v'')\ R_e^2(\bar{r})\ q_{v'v''}}$$

$$= \frac{8\pi^3}{3h^2c} \frac{\left[\sum_{v''} N(X,v'')\ R_e^2(\bar{r})\ q_{v'v''}\ I_{\odot}(A,v';X,v'')\right]\ \nu^3(A,v';X,v'')\ R_e^2(\bar{r})\ q_{v'v''}}{\sum_{v''} \nu^3(A,v';\ X,v'')\ R_e^2(\bar{r})\ q_{v'v''}}$$

Hence the intensity of emission in the v' - v'' band is given by

$$I_{v'v''} = hc\ \nu(A,v';\ X,v'')\ a(v'-v'')$$

$$= \frac{hc\ g(v')\ \nu^4(A,v';\ X,v'')\ R_e^2(\bar{r})\ q_{v'v''}}{\sum_{v''} \nu^3(A,v';\ X,v'')\ R_e^2(\bar{r})\ q_{v'v''}}$$

This sequence of operations is repeated for any desired temperature.

Considerable choice remains as to what Franck-Condon factors $p(v'v'')$ are used. Of the theoretical calculations we have three choices

(1) Nicholls' values of $q(v'v'')$ based on the Morse potentials

(2) Sharma's values of $q(v'v'')$ based on the R.K.R. potentials

(3) Nicholls' values modified to allow for the variation of the electronic transition moment with r-centroid, according to the result of Tawde and Korwar [20] or the result of Hébert and Tyte. [22].

We may also calculate relative vibrational transition probabilities for the $A^2\Sigma - X^2\Sigma$ system using the published sets of relative intensities obtained from excitation of the Aℓ0 spectrum in the following sources

(1)	AC arc	Hébert and Tyte [21]
(2)	Exploding foil	Tyte and Hébert [22]
(3)	Shock Tube	Tyte and Hébert [22]

Sets of relative transition probabilities were obtained from the above sets of relative intensities by using the relationship

$$p(v'v'') = \frac{I(v'v'')}{\nu^4(v'v'')\, N(v')}$$

$N(v')$ is calculated assuming that the v' level populations attain a Boltzmann distribution at the published temperatures. Figure 7 shows the relative populations of the v' levels observed by Hébert and Tyte, along with curves corresponding to three different temperatures. In evaluating transition probabilities from this set of measurements, it was assumed that $N(v')$ conformed to the theoretical (straight-line) curve, rather than the observed set. This was done so as to make the treatment of the data identical to that of the other two sets of relative intensity measurements.

Temperatures of 400, 600, and 800°K were assumed. Tables 6a, 6b and 6c show the relative intensities of bands in the $\Delta v = 0, \pm 1$ sequences at these temperatures calculated for each of five sets of transition probabilities, three determined from relative intensity measurements, and two theoretical. These correspond to

(1)	AC arc	Experimental
(2)	Exploding foil	Experimental
(3)	Shock tube	Experimental
(4)	Morse potential curve (Nicholls)	Franck-Condon Factors
(5)	Experimental potential curve (Sharma)	Franck-Condon Factors

In Tables 7a and 7b we give the relative intensities of bands with the $\Delta v = \pm 1$ sequences, and also include for comparison the results of Authier [37]. This data is also given graphically in Figures 8a and 8b.

Discussion of these Results. As may be expected, the scatter in observed laboratory relative intensities leads to an equally large scatter in the plot of intensity ratio versus temperature. The $\Delta v = +1$ sequence has intensity ratios which are more sensitive to temperature, in agreement with the conclusion of Authier [37]. However, by comparing the curves labelled "Sharma" and "Nicholls," it may be seen that even very small changes in the relative vibrational transitions probabilities lead to significant changes in apparent temperature. In the range shown any intensity ratio converted to temperature using Nicholls' Franck-Condon factors will lead to a temperature which is about 40°K higher than that

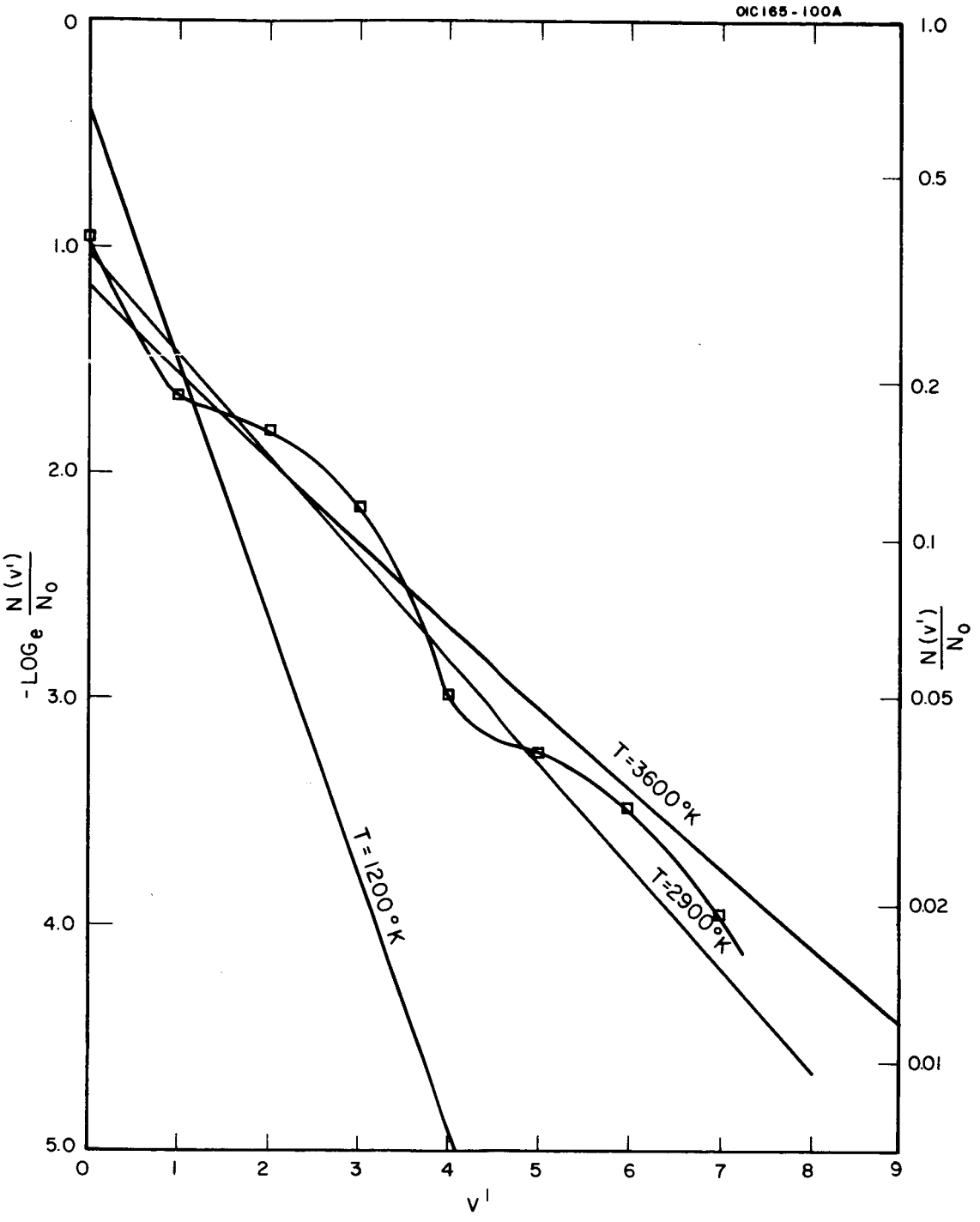

Figure 7. Relative population of vibrational levels in AC arc.

TABLE 6a

CALCULATED RELATIVE INTENSITIES OF $\Delta v = 0, \pm 1$ FLUORESCENCE BANDS AT $400^{\circ}K$ FOR SEVERAL SETS OF TRANSITION PROBABILITIES

$T = 400^{\circ}K$

	Arc			Foil		
v' \ Δv	+1	0	-1	+1	0	-1
0	--	100	9.661	--	100	39.56
1	10.73	8.689	8.385	29.29	30.92	26.90
2	2.039	0.3168	0.9992	14.09	8.246	10.46
3	0.2722	--	0.1448	0.6984	0.1916	0.5919
4	0.00745	--	0.00629	0.02630	--	0.02384
5	0.00083			0.00132		

	Shock		
v' \ Δv	+1	0	-1
0	--	100	23.64
1	21.33	12.48	22.18
2	5.153	0.7537	4.242
3	0.4718	--	0.3262
4	0.0267	--	0.0153
5	0.0013		

	Nicholls' F.C. Factors			Sharmas' F.C. Factors		
v' \ Δv	+1	0	-1	+1	0	-1
0	--	100	27.67	--	100	27.52
1	12.21	16.14	12.85	12.10	15.60	13.05
2	3.454	0	3.000	3.523	1.349	3.094
3	0.5001	--	0.4317	0.5328	--	0.4673
4	0.0550	--	0.0499	0.0699	--	0.06639
5	0.00531			0.00848		

TABLE 6b

CALCULATED RELATIVE INTENSITIES OF $\Delta v = 0, \pm 1$ FLUORESCENCE BANDS AT $600^{\circ}K$ FOR SEVERAL SETS OF TRANSITION PROBABILITIES

$T = 600^{\circ}K$

	Arc			Foil		
v' \ Δv	+1	0	-1	+1	0	-1
0	--	100	9.689	--	100	39.56
1	11.38	9.247	8.924	30.92	32.65	28.40
2	4.614	0.7170	2.261	16.004	9.367	11.88
3	0.8576	--	0.5592	2.293	0.6508	2.013
4	0.1738	---	0.06608	0.2652	---	0.2416
5	0.01828			0.02914		

	Shock		
v' \ Δv	+1	0	-1
0	--	100	23.64
1	22.11	12.94	22.99
2	7.161	1.047	5.894
3	1.651	---	1.148
4	0.2698	--	0.1543
5	0.02989		

	Nicholls' F.C. Factors			Sharmas' F.C. Factors		
v' \ Δv	+1	0	-1	+1	0	-1
0	--	100	27.67	--	100	27.520
1	13.24	17.51	13.93	13.11	16.89	14.12
2	4.869	2.194	4.230	4.949	1.895	4.346
3	1.093	0.1900	0.9439	1.136	0.1329	1.028
4	0.1987	0.01177	0.1827	0.2157	0.00368	0.2051
5	0.03274			0.03707		

TABLE 6c

CALCULATED RELATIVE INTENSITIES OF $\Delta v = 0, \pm 1$ FLUORESCENCE BANDS AT $800^{\circ}K$ FOR SEVERAL SETS OF TRANSITION PROBABILITIES

$T = 800^{\circ}K$

	Arc			Foil		
v' \ Δv	+1	0	-1	+1	0	-1
0	--	100	9.662	--	100	39.55
1	12.26	9.959	9.610	33.04	34.88	30.34
2	7.639	1.187	1.918	18.40	17.58	13.66
3	2.245	--	1.194	4.567	0.1227	3.870
4	0.5994	---	0.2280	0.8755	--	0.7977
5	0.1034			0.1602		

	Shock		
v' \ Δv	+1	0	-1
0	--	100	23.64
1	22.40	13.11	23.29
2	9.539	1.395	7.852
3	3.272	--	2.275
4	0.8895	--	0.5088
5	0.1490		

	Nicholls' F.C. Factors			Sharma's F.C. Factors		
v' \ Δv	+1	0	-1	+1	0	-1
0	--	100	27.67	--	100	27.52
1	14.55	19.24	15.31	14.39	18.54	15.50
2	6.607	2.940	5.742	6.643	2.562	5.876
3	2.002	0.3480	1.728	2.046	0.2394	1.798
4	0.5067	0.03000	0.4662	0.5215	0.00890	0.4950
5	0.1164			0.1167		

TABLE 7a

RELATIVE INTENSITIES IN $\Delta v = +1$ SEQUENCES

$T = 400^{\circ}K$

$v'-v''$	Arc	Foil	Shock	Nicholls	Sharma	Authier
1 - 0	100	100	100	100	100	100
2 - 1	19.068	48.102	24.159	28.286	29.112	28.100
3 - 2	2.546	2.384	2.212	4.096	4.40	0.4
4 - 3	0.070	0.090	0.125	0.451	0.58	
5 - 4	0.008	0.004	0.006			

$T = 600^{\circ}K$

$v'-v''$	Arc	Foil	Shock	Nicholls	Sharma	Authier
1 - 0	100	100	100	100	100	100
2 - 1	40.545	51.754	32.38	36.768	37.75	35.4
3 - 2	7.535	7.414	7.466	8.256	8.667	3.6
4 - 3	1.527	0.858	1.220	1.500	1.646	0.2
5 - 4	0.161	0.094	0.135	0.247	0.283	

$T = 800^{\circ}K$

$v'-v''$	Arc	Foil	Shock	Nicholls	Sharma	Authier
1 - 0	100	100	100	100	100	100
2 - 1	62.326	55.693	42.578	45.395	46.166	43.8
3 - 2	18.315	13.823	14.605	13.756	14.2215	12.9
4 - 3	4.891	2.650	3.970	3.482	3.625	0.9
5 - 4	0.843	0.485	0.665	0.800	0.811	

TABLE 7b

RELATIVE INTENSITIES IN $\Delta v = -1$ SEQUENCES

$T = 400^{\circ}K$

v'-v''	Arc	Foil	Shock	Nicholls	Sharma	Authier
0 - 1	100	100	100	100	100	100
1 - 2	86.796	67.981	93.826	46.437	47.41	46.7
2 - 3	10.343	26.432	17.945	10.843	11.241	11.0
3 - 4	1.498	1.496	1.380	1.560	1.70	
4 - 5	0.065	0.060	0.065		0.24	

$T = 600^{\circ}K$

v'-v''	Arc	Foil	Shock	Nicholls	Sharma	Authier
0 - 1	100	100	100	100	100	100
1 - 2	92.105	71.772	97.281	50.365	51.324	51.4
2 - 3	23.339	30.025	24.937	15.288	15.793	16.8
3 - 4	5.772	5.088	4.858	3.412	3.735	
4 - 5	0.682	0.611	0.653	0.661	0.745	

$T = 800^{\circ}K$

v'-v''	Arc	Foil	Shock	Nicholls	Sharma	Authier
0 - 1	100	100	100	100	100	100
1 - 2	99.462	76.697	98.554	55.354	56.337	56.4
2 - 3	19.853	34.526	33.219	20.755	21.352	22.2
3 - 4	12.354	9.784	9.627	6.247	6.534	
4 - 5	2.359	2.017	2.152	1.685	1.799	

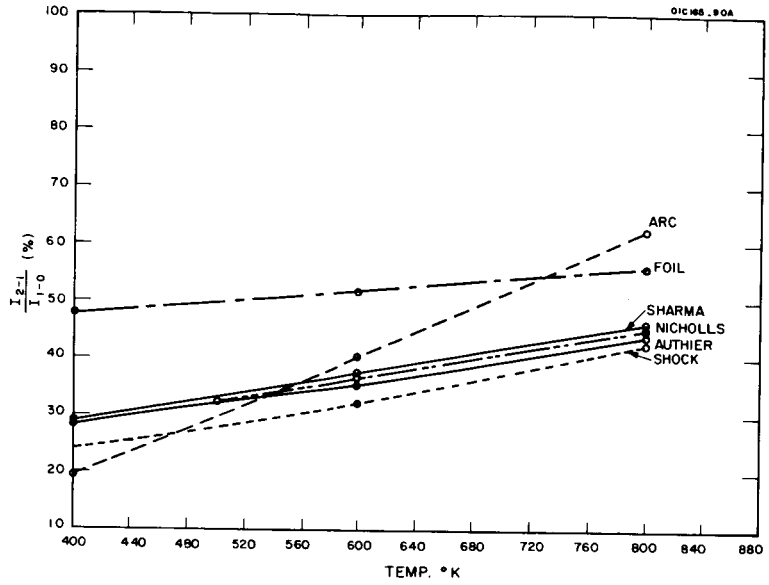

Figure 8a. Relative intensity of fluorescence bands in $\Delta v = +1$ sequence as a function of temperature.

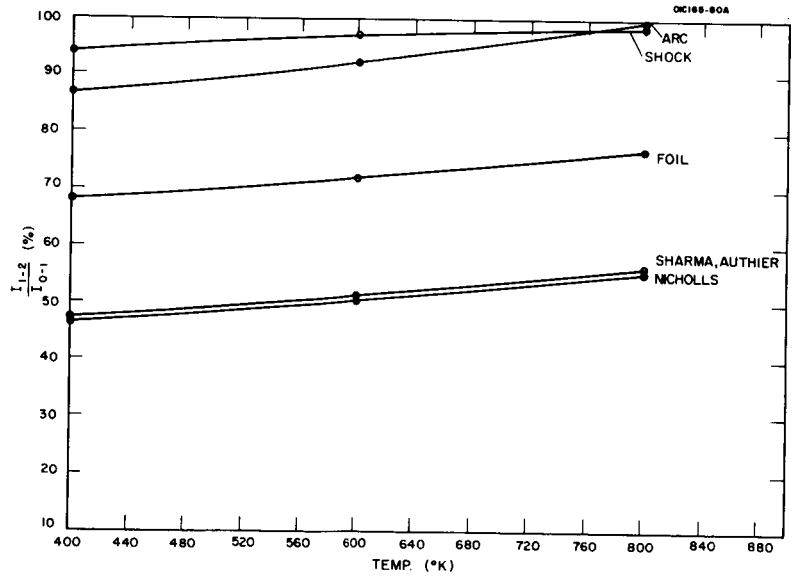

Figure 8b. Relative intensity of fluorescence bands in $\Delta v = -1$ as a function of temperature.

obtained using Sharma's Franck-Condon factors. Table 8 shows some of the ratios

$$\frac{q_{v'v''}\ (\text{Sharma})}{q_{v'v''}\ (\text{Nicholls})}$$

arranged in a Deslandres table with the Franck-Condon parabola underlined. It is seen that with one exception (4-3) agreement is within 2 percent along the two principal sequences. Examination of the values of $N(v'')\ p(v'v'')\ I_O(v'v'')$ obtained in the calculation of $g(v')$ shows that at 400°K the principal source for any excited v' level is $v'' = 0$, up to $v' = 3$. At 600°K the principal population sources are $v'' = 0 \rightarrow v' = 0,1,2$; $v'' 1 \rightarrow v' = 3$; $v'' = 2 \rightarrow v' = 4,5$. At 800°K the principal sources are $v = 0 \rightarrow v' = 0,1$; $v'' = 1 \rightarrow v' = 2,3$; $v'' = 2 \rightarrow v' = 4$; $v'' = 3 \rightarrow v' = 5$. Here the differences between the two sets of Franck-Condon factors are less than 10 percent.

Another potential source of error lies in the measurement of the intensity ratio

$$\frac{I_{2-1}}{I_{1-0}} = R$$

From Figure 7a it may be found that $dT/dR = 2325$; hence an intensity ratio error of 1 percent will lead to a temperature error of about 23°K.

The difference between the curves labelled "Nicholls" and "Authier" must be due entirely to the different solar spectrum used by Authier [37]. The latter used the solar spectral intensity measurements of Canavaggia [32]. These were made using light from the central spot of the solar disc, and, as has been shown in Figure 4, this has a relative intensity distribution which is higher at low wavelengths and lower at high wavelengths, compared to the data taken in light from the entire solar disc.

Authier also neglected the effects of Fraunhofer lines in the solar spectrum, although it has been shown that this may not be a serious source of error.

Conclusions. It is seen that three principal areas require detailed investigation before accurate temperatures may be obtained from the relative intensities of the vibrational bands of AℓO.

(1) The relative transition probabilities are as yet uncertain. The laboratory spectra used for this analysis should respond to the test for consistent relative intensities in a v'' progression. Most laboratory spectra have been obtained from hot sources in which the rotational structure is quite highly developed and therefore allowance has to be made for the degree of overlap

TABLE 8

RATIO OF FRANCK-CONDON FACTORS OBTAINED FROM ACTUAL AND MORSE POTENTIAL CURVES

v' \ v''	0	1	2	3	4
0	0.9999	0.9945	1.0339	1.2074	1.5193
1	0.9951	0.9697	1.0190	1.0588	1.2536
2	1.0102	1.0067	0.8660	1.0175	1.0827
3	1.1044	1.0635	0.9803	0.6597	0.9979
4	1.4871	1.2083	1.0705	0.9331	0.2695

among bands in any sequence. Correct values of the relative intensities in some of the v″ progressions should be obtained from the twilight fluorescence spectrum of Aℓ0, but this information may only be used to test the validity of laboratory spectra. The Franck-Condon factors of Sharma, being based on observed potential energy curves, are to be preferred over those of Nicholls. The differences between these two sets are slight, but serve to show the degree of accuracy required for $p_{v'v''}$. It is difficult to assume that the variation of R_e with $r_{v'v''}$ is small enough to ignore. Bates prediction [36] that it varys more slowly than as a first power of r for parallel-type transitions ($\Delta\Lambda = 0$) is not sufficiently accurate for our needs. At the moment it appears that if we accept the shock-wave excited laboratory spectra of Aℓ0 as being the most reliable, then the estimates of temperatures from vibrational spectra can be no more accurate than $\pm 100^{\circ}$K.

(2) The sensitivity of the calculated intensity ratios to the possible variants of the solar spectrum is not as high as might be anticipated. Nevertheless it is also obvious that for accuracies of better than $\pm 40^{\circ}$K, the solar spectrum, in integrated light, should be examined in some detail. This will become more apparent when we discuss the calculation of synthetic rotational spectra. We have already noted that few of the Fraunhofer lines coincide with features of the vibrational spectrum of Aℓ0, so that the effect on the peak intensities may be small. However the position of these peaks is sensitive to temperature, and the Fraunhofer lines may have an influence on integrated band intensities.

(3) We require to measure the relative intensities of the bands to an accuracy of about 1 percent for the 23 degree error in temperature. We have seen (Table 5) that the separation between band head and band origin is only 2-3Å. Although the bands are very similar in form (that is, head, peak populations etc occur at similar K-values from one band to the next) it should not be assumed that it is safe to consider relative intensities obtained with a bandwidth greater than 1Å. This may only be affirmed after testing by convolving several slit functions with several sythetic spectra. This of course requires a detailed investigation of the rotational structure of the electronic-vibration bands.

Calculation of Rotational Spectra

The mechanism for the population of the rotational levels of the $A^2\Sigma$ state is shown partially in Figure 9, the vibrational transitions for $\Delta v = 0, \pm 1$ only being shown for clarity. It may be seen immediately that the rate of population of any (A, v′,K′) rotational level is just as sensitive to error in the vibrational transition probabilities $p_{v'v''}$ as the rate of population of the (A,v′) vibrational level.

The rate of population of the level (A, v′, k′) is

$$g(A,v',K') = \sum_{v''}\sum_{K''} N(X,v'',K'')\, B(A,v',K';\, X,v'',K'')\, I_{\odot}(A,v',K';\, X,v'',K'')$$

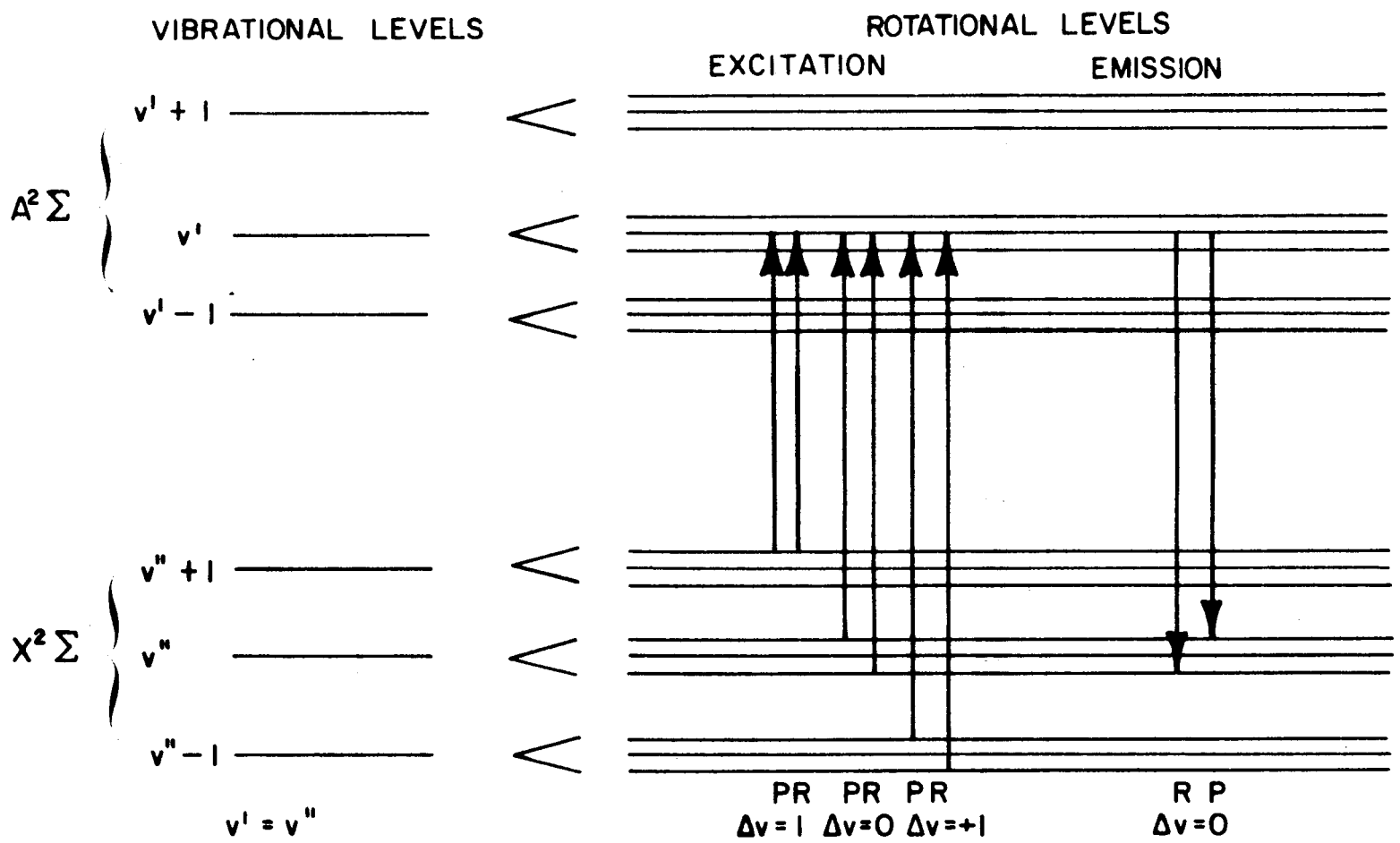

Figure 9. Excitation of rotational levels of $A^2\Sigma$ state.

We may express $B(A',v',K';\ X,v'',K'')$ as

$$B(A',v',K';\ X,v'',K') = \frac{8\pi^3}{3h^2c} R_e^2(\bar{r})\ q_{v'v''}\ S_{K'K''}$$

Hence

$$g(A,v',K') = \frac{8\pi^3}{3h^2c} \sum_{v''} \sum_{K''} N(X,v'',K'') R_e^2(\bar{r})\ q_{v'v''}\ S_{K'K''}\ I_{\odot}(A,v',K';X,v'',K'')$$

We have seen in Section III.C that $S_{K'K''} = 0$ unless $\Delta K = \pm 1$

Then, for $\Delta K = +1$ (R branch)

$$K' = K'' + 1 \text{ and } S_R = \frac{K'}{2K' - 1}$$

and, for $\Delta K = -1$ (P branch)

$$K' = K'' - 1 \text{ and } S_P = \frac{K' + 1}{2K' + 3}$$

Hence

$$g(A,v',K') = \frac{8\pi^3}{3h^2c} \sum_{v''} R_e^2(\bar{r})\ q_{v'v''} \left[N(X,v'',K'-1)\ \frac{K'}{2K'-1}\ I_{\odot}(A,v',K';\ X,v'',K'-1) \right.$$

$$\left. + N(X,v'',K' + 1)\ \frac{K' + 1}{2K' + 3}\ I_{\odot}(A,v',K';\ X,v'',K' + 1) \right]$$

The rate of depopulation of level (A,v',K') due to downward transitions is

$$a(A,v',K') = \sum_{v''} \sum_{K''} N(A,v',K')\ A(A,v',K';\ X,v'',K'')$$

$$= N(A,v',K') \sum_{v''} \sum_{K''} \frac{64\pi^4}{3h}\, \nu^3(A,v',K';\ X,v'',K'')\ R_e^2(\bar{r})\ q_{v'v''}\ S_{K'K''}$$

Referring again to Section III.C, $S_{K'K''} = 0$ unless $\Delta K = \pm 1$

Then for $\Delta K = +1$ (R branch)

$$K' = K'' + 1 \text{ and } S_R = \frac{K'}{2K' + 1}$$

and for $K = -1$ (P branch)

$$K' = K'' - 1 \text{ and } S_P = \frac{K' + 1}{2K' + 1}$$

Hence

$$a(A,v'K') = \frac{64\pi^4}{3h}\, N(A,v',K') \sum_{v''} R_e^2(\bar{r})\ q_{v'v''} \left[\nu^3(A,v',K';\ X,v'',K' - 1)\ \frac{K'}{2K' + 1}\right.$$

$$\left. + \nu^3(A,v',K';\ X,v'',K' + 1)\ \frac{K' + 1}{2K' + 1}\right]$$

At equilibrium $g(A',v',K') = a(A',v',K')$ and the population of the level (A,v',K') will be

$$N(A,v',K') = \frac{g(A,v',K')}{\frac{64\pi^4}{3h}\sum_{v''} R_e^2(\bar{r})\, q_{v'v''}\left[\nu^3(A,v',K';X,v'',K'-1)\,\frac{K'}{2K'+1} + \nu^3(A,v',K';X,v'',K'+1)\,\frac{K'+1}{2K'+1}\right]}$$

$$= \frac{1}{8\pi hc}\,\frac{\sum_{v''} R_e^2(\bar{r})\, q_{v',v''}\left[N(X,v'',K'-1)\frac{K'}{2K'-1}\, I_{\odot}(A,v',K';X,v'',K'-1) + N(X,v'',K'+1)\frac{K'+1}{2K'+3}\, I_{\odot}(A,v',K';X,v''K'+1)\right]}{\sum_{v''} R_e^2(\bar{r})\, q_{v'v''}\left[\nu^3(A,v',K';X,v'',K'-1)\frac{K'}{2K'+1} + \nu^3(A,v',K';X,v',K'+1)\frac{K'+1}{2K'+1}\right]}$$

Therefore the intensity of each rotational line in the R branch corresponds to the rate of photon emission in the transition $(A,v'K') \rightarrow (X,v'',K'-1)$

$$a(A,v',K';X,v''K'-1) = N(A,v',K')\ A(A,v',K';X,v'',K'-1)$$

$$= \frac{g(A,v'K')\ R_e^2(\bar{r})\ q_{v'v''}\ \nu^3(A,v',K';X,v''K'-1)\ \frac{K'}{2K'+1}}{\sum_{v''} R_e^2(\bar{r})\ q_{v'v''}\left[\nu^3(A,v',K';X,v''K'-1)\frac{K'}{2K'+1} + \nu^3(A,v'K';X,v'',K'+1)\frac{K'+1}{2K'+1}\right]}$$

and the intensity of the line $(A,v',K';X,v'',K'-1)$ of the R branch is

$$I(A,v'K';v''K'-1) = hc\ \nu(A,v',K';X,v'',K'-1)\ a(A,v',K';X,v''k'-1)$$

Similarly, the rate of photon emission in the P branch is

$$a(A,v',K';X,v'',K'+1) = N(A,v',K')\ A(A,v',K';X,v'',K'+1)$$

$$= \frac{g(A,v'K')\ R_e^2(\bar{r})\ q_{v'v''}\ \nu^3(A,v',K';X,v'',K'+1)\ \frac{K'+1}{2K'+1}}{\sum_{v''} R_e^2(\bar{r})\ q_{v'v''}\left[\nu^3(A,v',K';X,v'',K'-1)\frac{K'}{2K'+1} + \nu^3(A,v'K';X,v'',K'+1)\frac{K'+1}{2K'+1}\right]}$$

and the intensity of the line $(A,v',K';X,v''K'+1)$ of the P branch is

$$I(A,v',K';X,v'',K'+1) = hc\ \nu(A,v',K';X,v'',K'+1)\ a(A,v',K';X,v'',K'+1)$$

It is seen that the vibrational transition probabilities $p_{v'v''}$ occur twice in the numerator and once in the denominator of the expressions for the intensities of the R and P branches. If we are concerned only with the relative intensities within any one band (rotational profiles) then $p_{v'v''}$ occurs once each in both the numerator and the denominator. In order to predict accurately the effects of overlapping of adjacent bands we also require to know the values of $p_{v'v''}$ accurately; however this may be estimated by extrapolation of the observed band profiles.

Due to the lack of vibrational transition probabilities which may be used with confidence, the computation of synthetic rotational spectra, by the mathematical techniques which we have just given, may not be justified. Profiles of the $\Delta v = 0$ and $\Delta v = +1$ sequences using

$$p_{v'v''} \propto [1 - 0.46\ (\bar{r}_{v'v''})]^2\ q_{v'v''}$$

have been calculated by Harang[38].

The situation may be somewhat simplified if we make the following assumptions:

(1) The energy differences among the rotational levels within any vibrational level are reproduced exactly from one vibrational level to the next in each electronic state. We may then write

$$N(X,v'',K'') = N(X)\ N(v'')\ N(K'')$$

where

$$N(X),\ N(v'')$$

and

$$N(K'')$$

each correspond to a normal Boltzmann distribution. We have already seen that $N(X) = N_o$ for the range of temperatures to be encountered.

(2) The intensity of the sun, in energy per unit wave number interval, remains constant across both branches of each band, so that

$$I_\odot(A,v',K';X,v'',K'-1) = I_\odot(A,v',K';X,v'',K'+1) = I_\odot(A,v';X,v'')$$

(3) The dependence of the transition probability for spontaneous emission on wavelength, through

$$A_{nm} = \frac{64\pi^4}{3h}\ \nu_{nm}^3\ \left|R_{nm}\right|^2$$

will be ignored for any one band

Thus

$$\nu(A,v',K';X,v'',K'-1) \simeq \nu(A,v',K';X,v'',K'+1) \simeq (A,v';X,v'')$$

The rate of population of level (A,v',K') now becomes

$$g(A,v',K') = \frac{8\pi^3}{3h^2c} N_o \sum_{v''} N_{v''} R_e^2(\bar{r}) q_{v'v''} I_{\odot}(A,v';X,v'') \left[N(K'-1)\frac{K'}{2K'-1} + N(K'+1)\frac{K'+1}{2K'+3}\right]$$

This makes the relative rates of population of each K' level independent of the particular v' level concerned. Again in emission, since the relative line strengths depend only on the values of K' and K'', all bands will be expected to have the same shape.

Since the lines are fairly close and may not be resolved, we introduce another approximation by putting

$$N(K'-1) \simeq N(K'') \simeq N(K'+1)$$

$$g(K') = \frac{8\pi^3}{3h^2c} N_o \sum_{v''} N_{v''} R_e^2(\bar{r}) q_{v'v''} I_{\odot}(A,v';X,v'') \left[\frac{K'}{2K'-1} + \frac{K'+1}{2K'+3}\right] N(K'')$$

$$= \frac{8\pi^3}{3h^2c} N_o N(K'') \left[\frac{4K'^2 + 4K' - 1}{4K'^2 + 4K' - 3}\right] \sum_{v''} N_{v''} R_e^2(\bar{r}) q_{v'v''} I_{\odot}(A,v';X,v'')$$

$$\simeq \frac{8\pi^3}{3h^2c} N_o N(K'') \sum_{v''} N_{v''} R_e^2(\bar{r}) q_{v'v''} I_{\odot}(A,v';X,v'')$$

The rate of depopulation of levels K′ becomes a(K′)

$$a(K') = \frac{64\pi^4}{3h} N_{v'} N_{K'} \left[\frac{K'}{2K'+1} + \frac{K'+1}{2K'+1}\right] \sum_{v''} R_e^2(\bar{r})\, q_{v'v''}\, \nu^3(A,v';X,v'')$$

$$= \frac{64\pi^4}{3h} N_{v'} N_{K'} \sum_{v''} R_e^2(\bar{r})\, q_{v'v''}\, \nu^3(A,v';\ X,v'')$$

At equilibrium $g(K') = a(K')$ and

$$N_{K'} = \frac{g(K')}{\frac{64\pi^4}{3h} N_{v'} \sum_{v''} R_e^2(\bar{r})\, q_{v'v''}\, \nu^3(A,v';\ X,v'')}$$

$$= \frac{1}{8\pi hc} \frac{N_o\, N(K'') \sum_{v''} N_{v''}\, R_e^2(\bar{r})\, q_{v'v''}\, I_{\odot}(A,v';\ X,v'')}{N_{v'} \sum_{v''} R_e^2(\bar{r})\, q_{v'v''}\, \nu^3(A,v';\ X,v'')}$$

It may be seen that the relative populations of the K′ levels follows exactly that of the K″ levels. It is as if they were arranged in a Boltzmann distribution also.

Thus the rate of photon emission in the R branch is proportional to

$$a(K')_R = N(K'') \frac{K'}{2K + 1}$$

and in P branch is

$$a(K')_P = N(K'') \frac{K' + 1}{2K' + 1}$$

In both the above we put $K'' = K'$ for the purpose of evaluating $N(K'')$. An approximate method has been used by Low [39] which gives a result similar to this.

VALIDITY OF SYNTHETIC SPECTRA

Vibrational and Rotational Relaxation

The processes described mathematically in the preceding sections are valid for only one cycle of the excitation-emission process. It is assumed that when the cycle is repeated, the population distribution of the vibrational and rotational levels is again in thermal equilibrium with the surrounding atmosphere. More briefly, vibrational and rotational relaxation should be complete. When the time between consecutive excitations is long compared with the time between collisions, this will certainly be the case. Although the number of collisions necessary for complete relaxation is uncertain, it may be estimated from a comparison with other diatomic molecules. If the time between collisions is very much longer than the time between excitations, then the population distributions of the vibrational and rotational levels will tend to be in thermal equilibrium with the solar energy flux; that is, the apparent temperature will approach 6000°K. The actual situation lies somewhere between two extremes.

Vibrational levels of the lower electronic state ($v'' \geq 1$) may be depopulated either by collisions with other molecules, or by the spontaneous emission of infrared radiation. In the latter case the equilibrium distribution will be determined by the infrared radiation from the sun and from the earth. The transfer of energy in heteromolecular collisions is slow, except when there is a similarity in the vibrational energy levels of the two colliding molecules [40]. The vibrational energy quantum of the prevalent atmospheric molecule, N_2, is much greater than that of AlO. Vibrational relaxation is also relatively rapid when the non-relaxing molecule is light (for example, H_2 or He_2) [41], but this will not apply to trails of AlO generated in the altitude range presently being considered. The number of collisions necessary for vibrational relaxation is certainly not less than 10^4 and may be as great as 10^8.

From the intensity of the AlO trail, it would appear that one excitation occurs every 1 to 10 seconds, in which time, at 140 km, 33 to 330 collisions will have occurred. At 110 km, the number of collisions between excitations will be 540 to 5400. Thus it is not safe to assume that vibrational relaxation is complete above 110 km.

In the case of rotational relaxation, since the energy involved is small, relatively few - perhaps 10 to 20 - collisions are necessary [42]. Therefore it should be safe to assume that rotational relaxation is complete up to about 200 km, where the collision frequency is about 5 sec^{-1}.

Polarization of the Bands

It has been shown [1,2] that for large J-values, the degree of polarization P of the vibration rotation bands excited by natural (unpolarized) light, tends to 1/7 for the R and P branches, for large value of J. The degree of polarization is defined as

$$P = \frac{I_{\parallel} - I_{\perp}}{I_{\parallel} + I_{\perp}}$$

Any vibrational-rotational level may be populated and depopulated by transitions corresponding to the R and P branches. Thus there are four cases to be considered. The degrees of polarization are given by Feofilov [2] and are:

$$P_{R\to R} = \frac{(J + 2)(2J + 5)}{14J^2 + 23J + 10}$$

$$P_{R\to P} = \frac{1}{7}$$

$$P_{P\to R} = \frac{1}{7}$$

$$P_{P\to P} = \frac{(J - 1)(2J - 3)}{14J^2 + 5J + 1}$$

For

$$J = 10,\ 1/2\ (P_{R\to R} + P_{P\to R}) = 0.163$$

and

$$1/2(P_{R\to P} + P_{P\to P}) = 0.124$$

and at

$$J = 20,\ 1/2(P_{R\to R} + P_{P\to R}) = 0.153$$

and

$$1/2(P_{R\to P} + P_{P\to P}) = 0.133$$

Consequently, if the band profiles are measured with an instrument which is sensitive to the state of polarization of the incident radiation, the recorded relative intensities may not correspond exactly to the actual relative intensities. It is known that diffraction grating spectrometers are, in general, sensitive to the state of polarization of the incident radiation. Tests carried out on the Fastie 0.5-meter spectrometer using a tungsten lamp and a polarizer showed that over the wavelength range 4600 to 5200Å, the response was insensitive to the state of polarization. Therefore no further consideration of the polarization of the bands of the $\Delta v = 0, \pm 1$ sequences need be entertained here. The form of the polarization will be substantially the same from one band to the next, and will only affect the apparent rotational profiles, with a polarization-sensitive instrument. In any case the relative intensities of the bands, whether peak or integrated, should be independent of this, unless the relative sensitivity of the spectrometer to the two forms of polarization varies considerably over the 600Å range considered. The effect over any one band sequence is probably negligible.

ANALYSIS OF DATA OBTAINED FROM TRAIL OF Aℓ0 LAID AT FORT CHURCHILL
September 1966

Nike-Apache, No. 14-280, was launched at 01.22 GMT 16 September 1966 and ejected 1.75 kg TMA on the downward leg, covering the altitude range 181 km to 95 km. The time of TMA ejection was +248.4 and the spectrometer picked up the Aℓ0 spectrum at +280 sec. Spectra were obtained from this time to +2710 sec when the equipment was turned off. Spectra of the top 20 km of the trail could have been obtained for some 15 minutes following turn-off, but the spectrometer had to be modified for the observation of the continuum radiation expected from the next trail (14.281) and the countdown for this was already at T-52 minutes.

During the period of observation the upper part of the trail drifted toward a region of auroral activity (rayed band) and for one or two minutes the two features were visually overlapped (the auroral emission probably took place at lower altitudes, although the possibility of sunlit auroral rays can not be excluded). A spectrum of the aurora alone was also taken for control purposes. The auroral activity increased over the entire sky during the period for which the trail was observed.

Instrumentation

The spectrometer used for these observations was the 0.5-meter "Blue" instrument kindly made available by W.G. Fastie of the Johns Hopkins University, Baltimore. Although a description of this instrument has been given in the literature [43] the necessary details will be given here:

Focal length	50.0 cm
Grating	10 x 10 cm, 1200 ℓ/mm
Slit circle radius	7.5 cm
Slit length	4.45 cm
Photomultiplier	EMI Type 9558B (S-20 cathode)
Telescope aperture	12.382 cm
Telescope focal length	61.277 cm

If θ is the angle the grating normal makes with the axis the following characteristics apply in the wavelength region of interest

Wavelength (Å)	θ	Reciprocal Dispersion (Å/mm)
4600	16° 12.3′	15.14
4916	17° 21.2′	15.00
5200	18° 23.3′	14.86

Most spectra were taken with a resolution of 2.06Å; a few were taken at 5.21Å. The spectrum was recorded on a two channel chart recorder, moving at 1 cm/sec. The range covered was from 4576.6 to 5284.1Å giving a scan rate of 12.115Å/sec. During flyback the two channels were automatically switched to record the high voltage and slit settings. The latter were maintained to give large scale readings on the $\Delta v = \pm 1$ sequences with the 1X channel. This resulted in the 0 - 0 band overloading this channel, but the outputs could be scaled from the 10X channel. One or two spectra were recorded without the $\Delta v = 0$ sequence overloading the 1X channel so that accurate values of the relative intensities in the v″ progressions might be determined. These are of interest in order to check the validity of laboratory spectra. Only marked features of the trail were examined so that the temperatures obtained could be given a definite height. These corresponded to altitudes of 165, 140, 124, and 95 km. At 95 km the spectrum also contained a considerable amount of continuum, as might be expected from visual observation.

Temperatures

Most of the spectra were taken at the 165 km level and the analysis of data from this altitude has been carried out in several different ways:

(1) For each scan, relative intensities in the $\Delta v = \pm 1$ sequences may be converted directly to temperature. In this way 76 temperature values were obtained, from 558 to 1900°K. This range was divided into 100°K intervals and the frequency of occurence of a temperature in each interval was noted. Two maxima were obtained, of equal amplitude, in the regions 1001 to 1100°K and 1201 to 1300°K. Dividing the observation into three successive time periods showed this distribution on a smaller scale, so that there is no evidence here for any temperature change with time. Consequently it must be assumed that the heating effect produced by incoming auroral particles has a time constant longer than 35 minutes. On the other hand, when the arithmetic mean of the individual temperatures is calculated for each time period, we obtain 1082, 1131, and 1213°K, which does indicate a steady trend. The average of all 76 readings is 1139°K. It should be noted that this method of analysis weighs data equally, regardless of signal-to-noise quality.

(2) In each sequence the intensity ratios were normalized and added, in order to derive an average intensity ratio before converting to temperature. Again the data are weighed equally. The resulting average intensity ratios are then converted into temperature. The results are given in Table 9.

(3) In this the actual intensities of each band are added numerically for each group of scans. This has the effect of averaging out the noise and weighing each intensity ratio according to its absolute value. The ratio of the relative intensity totals is then converted into temperature. These results are also presented in Table 9.

It appears that the mean temperature at the 165 km level is about 1130°K during the observation and that a rate of increase of 7 ± 2°K/min was detected. For the entire 35-min sequence of observations, auroral activity increased and ultimately the Aℓ0 glow and auroral rays were superposed. Observations showing contamination by auroral emission features were exluded from results shown in Table 9.

TABLE 9

TEMPERATURES AT 165 KM

Scans	Δv = + 1 Sequence				Δv = - 1 Sequence				Average	
	Unweighted (2)		Weighted (3)		Unweighted (2)		Weighted (3)			
	$\frac{I_{2-1}}{I_{1-0}}$	$\frac{I_{3-2}}{I_{1-0}}$	$\frac{I_{2-1}}{I_{1-0}}$	$\frac{I_{3-2}}{I_{1-0}}$	$\frac{I_{1-2}}{I_{0-1}}$	$\frac{I_{2-3}}{I_{0-1}}$	$\frac{I_{1-2}}{I_{0-1}}$	$\frac{I_{2-3}}{I_{0-1}}$	All	Principal
1-16	866	1139	836	1089	1192	1089	1182	1077	1059	1019
17-28	879	1430	963	1476	1260	1175	1221	1048	1181	1081
29-35	1055	~1800	1035	~1750	1164	1057	1271	1062	1274	1131

The individual temperature determinations made at other altitudes are shown in Figure 10. The numbers beside them indicate the order of occurrence of the scans concerned. The arrows indicate upper limits, in that some of the intensity ratios observed were too low to be converted into a temperature. In this case the average of the other temperatures deduced for this altitude is treated as an upper limit.

Discussion of Results

It is seen that in all cases below 165 km the temperatures obtained are somewhat higher than either of the two standard atmospheres. However this is not unexpected, since the conditions were just those required for heating of the upper atmosphere. From 80 to 100 km the Kellogg hypothesis [44] is that the poleward migration of atomic oxygen and subsequent recombination can lead to heating of the polar winter mesosphere. It has been shown by Young and Epstein [45] that this process is capable of explaining a temperature rise of 100°K/day.

At higher altitudes, the atmosphere is subject to heating by the thin extension of the solar corona which surrounds the earth, as suggested by Chapman [46]. The earth's magnetic field can shield the upper atmosphere at temperate latitudes from this input, but near the poles the energetic protons can penetrate much closer to the surface of the earth, also causing aurorae. The possibility of heating by incoming auroral particles has already been suggested by Kellogg [44].

Although the lack of certainty concerning the transition probabilities renders the temperatures determined here to have a tolerance of as much as $\pm 150^{\circ}$K, it is seen that the points obtained do converge to about 200°K at 100 km, as required. Certainly the rate of rise of temperature with both time and altitude may be regarded as valid since the most probable Intensity Ratio versus Temperature plots (Figures 8a and 8b) have the same slope.

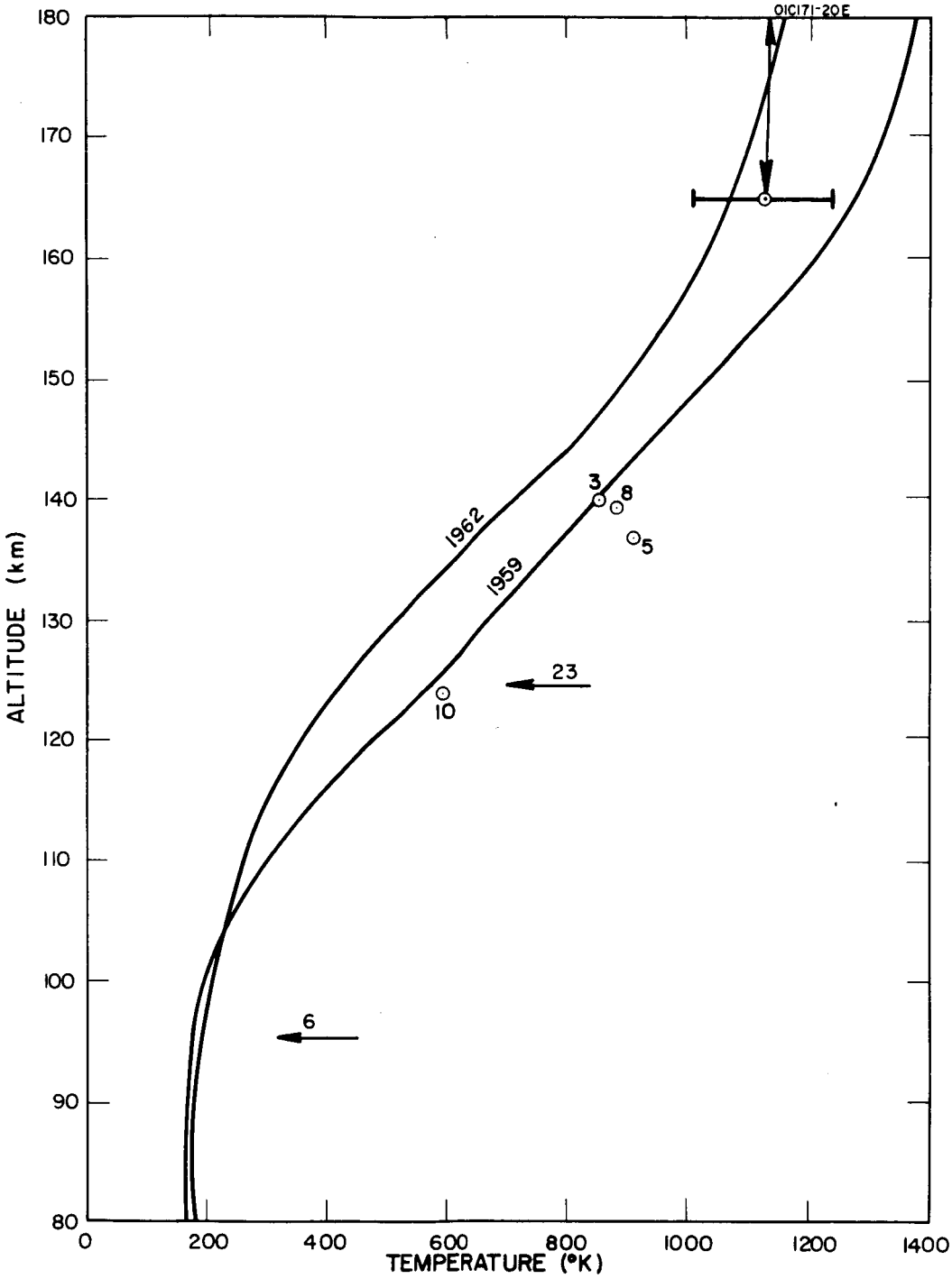

Figure 10. Upper atmosphere temperatures deduced from spectrum of Aℓ0 fluorescence at Fort Churchill, October 1966.

Since the cloud was quite diffuse at the 165 km level, and had a diameter of about 20 km, it probable that the temperature data obtained from this region corresponds to the altitude range from 165 to 180 km, as indicated in Figure 10.

Analysis of the electron temperature data from both flights, 14.280 and 14.281, show that the electron temperature at 170 km is about 1150°K, and at 180 km is about 1375°K. Although the data from both these flights were in fair agreement the first set of data was taken just at the beginning of the buildup of auroral activity and the second set after some 40 minutes of negligible activity. The auroral activity ceased shortly after the termination of the spectrometer observations.

Relative Intensities in ($v' = 1$) v'' Progression

The relative intensities among the bands in any v'' progression should be the same regardless of the method of excitation, provided that the source of these bands is optically thin. Therefore the relative intensities of bands in the v'' progressions observed at twilight should be examined in order to have a standard by which to judge the validity of laboratory spectra.

The v'' progression with $v' = 0$ was not analyzed at this time due to the overloading of the recorder by the 0 - 0 band. This was delibertely done so as to get accurate measurements of the $\Delta v = \pm 1$ sequences. Moreover the 0 - 0 band is probably optically thick, particularly during the first few minutes [47] and thus true relative intensity measurements would be difficult.

Of the v'' progression with $v' = 2$, only the 2-1 band is observed. The 2-0 band is outside the range of observation, and 2-2 band to too weak to be measured accurately. In fact it was only detected on two scans, both at the top of the trail, as may be expected.

Thus only the v'' progression with $v' = 1$ received much attention. Again the analysis was carried out in two ways, weighting the relative amplitudes and leaving them unweighted. The results are shown in Table 10 in terms of photon intensity $a_{v',v''}$.

TABLE 10

RELATIVE INTENSITIES IN v'' PROGRESSION $v' = 1$

Band	1-0	1-1	1-2
Weighted $a_{v',v''}$	60.92	100	83.77
Unweighted $a_{v',v''}$	66.38	100	76.38
Sharma $\nu_{v',v''}\ \nu^3$	74.10	100	87.60

Also given in Table 10 is the relative photon intensity expected on the basis of Sharma's [19] Franck-Condon factors above. The lack of agreement is apparent. Only bands with $v'' = 0$ should suffer self-absorption to any appreciable extent. Again it is obvious that there is still much uncertainty concerning the actual transition probabilities.

CONCLUSIONS AND RECOMMENDATIONS FOR FUTURE WORK

The apparent rise in temperature during a build up in auroral activity is an interesting observation. Before any firm conclusions are reached it would be desirable to perform similar experiments under the following three conditions. (1) Build-up of auroral activity at morning twilight, (2,3) Decline in auroral activity at morning and evening twilight.

Observations from latitudes not so close to the auroral zone are also desirable, although it would be interesting to see if a similar effect occurred during moderate latitude aurorae.

As far as the Aℓ0 fluorescence method of temperature determination is concerned, it is obvious that the technique requires major attention to be given in three areas.

(1) The signal-to-noise ratio of the present observations is low, as evidenced by the scatter in 76 temperatures obtained at the 165 km level. A larger throughput may only be obtained by using a larger instrument, without sacrificing resolution. However, in order to measure integrated band intensities accurately requires more resolution because of the overlapping of adjacent bands. For rotational temperatures again better resolution is required. The sighting arrangements in use also require some improvement, as it is not possible to optimize the field of view of the spectrometer with respect to the trail. Exploration of fine structure of the temperature profile may require that the slit be oriented across, rather than along the trail. If the field of view of the spectrometer is to be defined by the entrance slits and a telescope, the focal length of the spectrometer should be as large as 1.5 to 2.0 meters with the gratings now available. Alternatively the field of view could be determined by the grating itself allowing a longer focal length and higher resolution. The advantages of both systems should be considered before making a decision. For further investigation of the Aℓ0 spectrum in the laboratory it may be desirable to use photographic recording of the spectra, due to the fluctuating (or transient) nature of the source. The same instrument could perform both tasks if constructed as suggested by Mielenz [48].

(2) The relative intensities and fine structure of the spectrum of the integrated solar disc should be investigated, and at wavelengths outside the region 4600 to 5200Å, since significant rates of population of the v' levels occur in the $\Delta v = \pm 2,3$ sequences, under certain conditions. These measurements should be on an absolute scale, and extrapolated to zero air-mass.

(3) The vibrational transition probabilities in the $A^2\Sigma$ to $X^2\Sigma$ sequence of Aℓ0 are very uncertain. Laboratory experiments are required in order to resolve this, and several spectra displaying consistent relative intensities in the v' progressions are required.

Several alternative methods of temperature measurement are worth considering, and it is suggested that the following topics be investigated.

(1) The release of barium vapor into the upper atmosphere leading to the observation of BaI and BaII atomic lines is noted. The spectrum of BaO is very similar to that of AℓO, being $^1\Sigma - \Sigma'$, and lies at 6000Å. It might be possible to observe resonance radiation doppler line widths for both the neutral atom and the ion, and at the same time obtain fluorescence spectra of the oxide. It has also been reported [49] that many lines other than the resonance lines of BaI and BaII are excited. This data should be examined to see if any bright lines are available for which the lower state is not the ground state. This would allow determination doppler widths of lines free of self-absorption corresponding to the suggestion already made for lithium [50].

(2) The possibility of observing purely rotational transitions of AℓO is attractive. These would lie at approximately 38.5G c/s and its harmonics. Inspection of Figure 6 shows that the relative populations of the $K'' = 0$, 1 and 2 rotational levels are very sensitive to temperature. If a suitable radar system were used to irradiate the cloud of AℓO with pulses of rf energy at 38.5 Gc/s and its harmonics, then the relative amplitudes of the return pulses would indicate the relative populations of the lower rotational levels. It is not suggested that this is the best system to use. Obviously the transition probability will be very small due to the ν^3 effect, but a search should be made for a suitable molecule which will give a satisfactory response with available rf technology. The radar method has the advantage of not being dependent on dark skies or on sunlight for irradiation, and could thus be used during daylight, twilight, and nighttime for both positional (winds) and temperature purposes. In searching for alternative ejectable molecules, advantage should also be taken of the capabilities of pulsed optical lasers in the visible and infrared which might excite vibrational or even electronic transitions. Here, of course, the daytime background is no longer insignificant. Attention is also drawn to the fact that many triatomic molecules have rotational spectra in the region 3 to 10 G c/s [51]. The frequency band 10 to 400 Gc/s may be excluded due to atmospheric opacity.

REFERENCES

1. Herzberg, G., "Molecular Spectra and Molecular Structure I - Spectra of Diatomic Molecules", second ed., Van Nostrand, New York (1950).

2. Feofilov, P.P., "The Physical Basis of Polarized Emission", Moscow, (English Translation Consultant's Bureau, New York 1961) (1950).

3. Soshnikov, V.N., "Absolute Intensities of Electronic Transitions in Diatomic Molecules", Usp Fiz. Nauk 74, 61, (Soviet Physics Uspekhi, 4, No. 3, November-December 1961) (1961).

4. Mulliken, R.S., "The Interpretation of Band Spectra, Part IIc, Empirical Band Types", Rev. Mod. Phys 3, 89 (1931).

5. Lagerqvist, A., N.E.L. Nilsson, and R F. Barrow, "Rotational Analysis of the $^2\Sigma$ - $^2\Sigma$ System of AℓO", Arkiv for Fysik 12, 543 (1957).

6. Sen, M.K., "Spin Doubling in $^2\Sigma$ States in AℓO", Indian J. Phys 11, 251 (1937).

7. Pomeroy, W.C., "The Quantum Analysis of the Band Spectrum of Aluminum Oxide (λ5200 - λ4650)", Phys. Rev. 29, 59 (1927).

8. Jevons, W. "Report on Band Spectra of Diatomic Molecules", The Phys. Soc. (1932).

9. Eriksson,G., and E. Hulthen, "Uber die Bandenspektra von Aluminium", Zeits f Physik 34, 775 (1925).

10. Roy, D., "New Measurements of Aluminium Monoxide Bands", Indian J. Phys. 13, 231 (1939).

11. Shimauchi, M., "Arc Spectra of Pure Aluminum in Various Gases", Science of Light 7, 101 (1958).

12. Manneback, C., "Computation of the Intensities of Vibrational Spectra of Electronic Bands in Diatomic Molecules", Physics 17, 1001 (1951).

13. Manneback, C. and A. Rahman, "Computation of Intensities of Vibrational Spectra of Electronic Bands in Diatomic Molecules II", Physica 20, 497 (1954).

14. Armstrong, E.B., "Observations of Luminous Clouds Produced in the Upper Atmosphere by Exploding Grenades - II, Emission of AℓO Bands from Sunlit Clouds", Planet Space Sci. 11, 743 (1963).

15. Bates, D.R., "Relative Transition Probabilities in Band Systems of Diatomic Molecules", M.N. Roy Ast. Soc., 112, 614 (1952).

16. Nicholls, R.W., "Frank-Condon Factors to High Vibrational Quantum Numbers II: SiO, MgO, SrO, AℓO, VO, NO", J. Res. Nat. Bur. Std. (US) 66A, 227 (1962).

17. Tawde, N.R. and V.M. Karwar, "Franck-Condon Factors and r-Centroids for the Aluminium Monoxide $A^2\Sigma^+ - X^2\Sigma^+$ Band System", Proc. Phys. Soc. 80, 794 (1962).

18. Bates, D.R., "The Intensity Distribution in the Nitrogen Band Systems Emitted from the Earth's Upper Atmosphere", Proc. Roy. Soc. 196A, 217 (1949).

19. Sharma, A., "Franck-Condon Factors and r-Centroids of the $A^2\Sigma - X^2\Sigma$ Band System of AℓO", J. Quant. Spectrosc. Radiat. Transf. 7, 289 (1967).

20. Tawde, N.R. and V.M. Korwar, "Electronic Transition Moment Variation in Bands of AℓO ($A^2\Sigma - X^2\Sigma^+$) System", Proc. Nat. Inst. Sci. India 29A, 325 (1963).

21. Hebert, G.R. and D.C. Tyte, "Intensity Measurements on the $A^2\Sigma - X^2\Sigma$ System of Aluminium Oxide", Proc. Phys. Soc. 83, 629 (1964).

22. Tyte, D.C. and G.R. Hebert, "The Electronic Transition Moment of the $A^2\Sigma - X^2\Sigma$ System of AℓO", Proc. Phys. Soc. 84, 830 (1964).

23. Tawde, N.R. and V.M. Korwar, "Effective Vibrational Temperature as a Variant of Electronic Transition Moment AℓO ($A^2\Sigma^+ - X^2\Sigma^+$) Band System", Indian J. Pure and Appl. Physics 3, 198 (1965).

24. Tyte, D.C., Private Communication (1966).

25. Tyte, D.C., "The Effect of Environmental Conditions on Band Strength", J. Quant. Spectrosc. Radiat. Transfer 5, 545 (1965).

26. Minnaert, M., G.F.W. Mulders, and J. Houtgast, "Photometric Atlas of the Solar Spectrum", Amsterdam (1940).

27. Priester, W., "Photometric von Fraunhofer-Linien mit der Lummer-Platte, angewandt auf die Mitte-Rand-Variation der Natrium D-Linien", Zt. fur Astrophys. 32, 200 (1953).

28. Dunkelman, L. and R. Scolnik, "Solar Spectral Irradiance and Vertical Atmospheric Attenuation in the Visible and Ultraviolet", J. Opt. Soc. Am. 49, 356 (1959).

29. Stair, R. and R.G. Johnston, "Preliminary Spectroradiometric Measurements of the Solar Constant, J. Res. Natl. Bur. Std. (US), 57 205 (1956).

30. Johnson, F.S., "The Solar Constant," J. Meteorol. 11, 431 (1954).

31. Johnson, F.S., J.D. Purcell, R. Tousey, and N. Wilson, "The Ultraviolet spectrum of the Sun," In "Rocket Exploration of the Upper Atmosphere" (Boyd, R.L.F., and Seaton, M.J. Editors) p279, Pergamon Press, London (1954).

32. Canavaggia, R., D. Chalonge, M. Egger-Moreau, and H. Oziol-Peltey, "Recherches Sur Le Spectre Continu du Soleil III ; Spectre continu de centre du disque entre 3200 et 5000Å," Ann d'Astrophys. 13, 355 (1950).

33. Labs, D., "Die Intensitat des kontinuierlichen Spektrums der Sonnemitte im Wellenlangenbereich $3300 \leqq \lambda \leqq 6900$Å," Zt. fur Astrophys. 44, 37 (1957).

34. Allen, C.W., "Astrophysical Quantities," London, Athlone Press (1955).

35. Tyte, D.C. and R. Nichols, "Identification Atlas of Molecular Spectra - 1 The AlO $A^2\Sigma - X^2\Sigma$ Blue-Green System," London, Ontario (1964).

36. Bates, D.R., "The Intensity Distribution in the Nitrogen Band Systems Emitted from the Earth's Upper Atmosphere," Proc. Roy. Soc. 196A, 217 (1949).

37. Authier, B., "Mesures De Temperature De L'Ionosphere A Partir De La Fluorescence De Molecules Produites Artificiellement Au Moyen De Fusees," Ann. de Geophys. 20, 353 (1964).

38. Harang, O., "AlO Resonant Spectrum for Upper Atmosphere Temperature Determination," Environmental Research Papers, No. 192, AFCRL-66-314, OAR, USAF (1966).

39. Low, C.H., "Atmospheric Temperature Measurement Above 100 km Altitude from AlO Spectra, "Planet Space Sci. 15, 199 (1967).

40. Lipscomb, F.S., R.G.W. Norrish, and B.T. Thrush, "The Study of Energy Transfer by Kinetic Spectroscopy - I. The Production of Vibrationally Excited Oxygen," Proc. Roy. Soc. 233A, 455 (1956).

41. Holmes, R., F.A. Smith, and W. Tempest, "The Vibrational De-Excitation of Oxygen in Heteromolecular Collisions," Proc. Phys. Soc. 83, 769 (1964).

42. Lambert, J.D., "Atomic and Molecular Processes," (Ed. D.R. Bates) p 783, Academic Press, New York (1962).

43. Fastie, W.G., "Instrumentation for Far-Ultraviolet Rocket Spectrophotometry," J. Quant. Spectrosc. Radiat. Transfer 3, 507 (1963).

44. Kellog, W.W., "Chemical Heating Above the Polar Winter Mesopause in Winter," J. Meteorol. 18, 373 (1961).

45. Young, C. and E. Epstein, "Atomic Oxygen in the Polar Winter Mesosphere," J. Atmos. Sci. 19, 435 (1962).

46. Chapman, S., "The thermosphere - The Earth's Outermost Atmosphere," Chapt I of "Physics of the Upper Atmosphere," (Ed. J.A. Ratcliffe) New York (1960).

47. Authier, B., J.E. Blamont, and G. Carpenter, "Measurement of the Ionsphere Temperature Beginning with the Twilight Fluorescence of Aluminum Oxide," Ann. Geophys, 20, 342 (1964).

48. Mielenz, K.D.,"Theory of Mirror Spectrographs, III. Focal Surfaces and Slit Curvature of Ebert and Ebert-Fastie Spectrographs," J. Res. Natl. Bur. Std. (US) 68C, 205 (1964).

49. Fastie, W.G., Private Communication, March (1967).

50. Best, G.T. and T.N.L. Patterson, "Temperature Determinations From a Cloud of Alkali Vapour in the Upper Atmosphere," Planet. Space Sci. 9, 521 (1962).

51. Kikuchi, C. and R.D. Spence "Microwave Methods in Physics, I. Microwave Spectroscopy," Am. J. Phys. 17, 288 (1949).